Endoscopy. Japan Gastroenterological Endoscopy Society (ed.). Tokyo: Igaku Shoin, 1999. (in Japanese.)
2 Ogoshi K, Kaneko E, Tada M *et al.* Japan Gastroenterological Endoscopy Society Risk Management Committee. Use of anticoagulants and antiplatelet agents during endoscopic procedures. *Gastroenterol. Endosc.* 2005; **47**: 2691–5. (in Japanese.)
3 Japan Gastroenterological Endoscopy Society Postgraduate Education Committee. *Guidelines for Gastroenterological Endoscopy version 3*. Japan Gastroenterological Endoscopy Society (ed.). Tokyo: Igaku Shoin, 2006. (in Japanese.)
4 2008 Report of Joint Study Group. Guidelines on anticoagulant and antiplatelet therapy for cardiovascular illnesses 2009 revised edn. (in Japanese.) Available from URL: http://www.j-circ.or.jp/guideline/pdf/JCS2009_hori_d.pdf
5 Joint Guidelines Committee on Strokes. *2009 Stroke Therapy Guidelines*. Shinohara Y, Ogawa A, Suzuki N, Katayama Y, Kimura A (eds). Kyowa Kikaku, 2009. (in Japanese.)
6 Anderson MA, Ben-Menachem T, Gan SI *et al.* Guidelines: Management of antithrombotic agents for endoscopic procedures. *Gastrointest. Endosc.* 2009; **70**: 1060–70.
7 Becker R, Scheiman J, Dauerman HL *et al.* Management of platelet-directed pharmacotherapy in patients with atherosclerotic coronary artery disease undergoing elective endoscopic gastrointestinal procedures. *Am. J. Gastroenterol.* 2009; **104**: 2903–17.
8 Bhatt DL, Scheiman J, Abraham NS *et al.* ACCF/ACG/AHA 2008 expert consensus document on reducing the gastrointestinal risks of antiplatelet therapy and NSAID use: A report of the American College of Cardiology Foundation Task Force on Clinical Expert Consensus Documents. *Circulation* 2008; **118**: 1894–909.
9 Veitch AM, Baglin TP, Gershlick AH *et al.* Guidelines for the management of anticoagulant and antiplatelet therapy in patients undergoing endoscopic procedures. *Gut* 2008; **57**: 1322–29.
10 Boustière C, Veitch A, Vanbiervliet G *et al.* Endoscopy and antiplatelet agents. European Society of Gastrointestinal Endoscopy (ESGE) guidelines. *Endoscopy* 2011; **43**: 445–58.
11 Shiffman RN, Shekelle P, Overhage JM *et al.* Standardized reporting of clinical practice guidelines: A proposal from the Conference on Guideline Standardization. *Ann. Intern. Med.* 2003; **139**: 493–8.
12 Eddy DM. Designing a practice policy: Standards, guidelines and options. *JAMA* 1990; **263**: 3077–82.
13 Ueno F, Matsui T, Matsumoto T *et al.* Evidence-based clinical practice guidelines for Crohn's disease, integrated with formal consensus of experts in Japan. *J. Gastroenterol.* 2013; **48**: 31–72.
14 Takada T, Hirata K, Mayuki T *et al.* Cutting-edge information for the management of acute pancreatitis. *J. Hepatobiliary Pancreat. Sci.* 2010; **17**: 3–12.
15 Becker RC, Scheiman J, Dauerman HL *et al.* American College of Cardiology & American College of Gastroenterology: Management of platelet-directed pharmacotherapy in patients with atherosclerotic coronary artery disease undergoing elective endoscopic gastrointestinal procedures. *J. Am. Coll. Cardiol.* 2009; **54**: 2261–76.
16 Sibon I, Orgogozo JM. Antiplatelet drug discontinuation is a risk factor for ischemic stroke. *Neurology* 2004; **62**: 1187–9.
17 Maulaz AB, Bezerra DC, Michel P *et al.* Effect of discontinuing aspirin therapy on the risk of brain ischemic stroke. *Arch. Neurol.* 2005; **62**: 1217–20.
18 Wahl MJ. Dental surgery in anticoagulated patients. *Arch. Intern. Med.* 1998; **158**: 1610–6.
19 Blacker DJ, Wijdicks EF, McClelland RL. Stroke risk in anticoagulated patients with atrial fibrillation undergoing endoscopy. *Neurology* 2003; **61**: 964–8.
20 Palareti G, Legnani C, Guazzaloca G *et al.* Activation of blood coagulation after abrupt or stepwise withdrawal of oral anticoagulants–a prospective study. *Thromb. Haemost.* 1994; **72**: 222–6.
21 Kaneko E, Munakata A, Iwao Y *et al.* Preventing complications associated with colonic endoscopy. *Gastroenterol. Endosc.* 2003; **45**: 1939–45. (in Japanese.)
22 Eisen GM, Baron TH, Dominitz JA *et al.* American Society for Gastrointestinal Endoscopy: Guidelines on the management of antithrombotic and antiplatelet therapy for endoscopic procedures. *Gastrointest. Endosc.* 2002; **55**: 775–9.
23 Sieg A, Hachmoeller-Eisenbach U, Eisenbach T. Prospective evaluation of complications in outpatients GI endoscopy: A survey among German gastroendoscopists. *Gastrointest. Endosc.* 2000; **51**: 37–41.
24 Parra-Blanco A, Kaminaga N, Kojima T *et al.* Hemoclipping for postpolypectomy and postbiopsy colonic bleeding. *Gastrointest. Endosc.* 2000; **51**: 37–41.
25 Whitson MJ, Dikman AE, von Althann C *et al.* Is gastroduodenal biopsy safe in patients receiving aspirin and clopidogrel? *J. Clin. Gastroenterol.* 2011; **45**: 228–33.
26 Shiffman ML, Farrel MT, Yee YS. Risk of bleeding after endoscopic biopsy or polypectomy in patients taking aspirin or other NSAIDS. *Gastrointest. Endosc.* 1994; **40**: 458–62.
27 Ono S, Fujishiro M, Hirano K *et al.* Retrospective analysis on the management of anticoagulants and antiplatelet agents for scheduled endoscopy. *J. Gastroenterol.* 2009; **44**: 1185–9.
28 Tono S, Morita Y, Miura M *et al.* Risks associated with endoscopic biopsy procedures undertaken while administering antiplatelet drugs. *Gastroenterol. Endosc.* 2011; **53**: 3326–35. (in Japanese.)
29 Ono S, Fujishiro M, Kanzaki H *et al.* Conflicting clinical environment about the management of antithrombotic agents during the periendoscopic period in Japan. *J. Gastroenterol. Hepatol.* 2011; **26**: 1434–40.
30 Yousfi M, Gostout CJ, Baron TH *et al.* Postpolypectomy lower gastrointestinal bleeding: Potential role of aspirin. *Am. J. Gastroenterol.* 2004; **99**: 1785–9.
31 Gerson LB, Triadafilopoulos G, Gage BF. The management of anticoagulants in the periendoscopic period for patients with atrial fibrillation: A decision analysis. *Am. J. Gastroenterol.* 2000; **95**: 1717–24.

32 Gerson LB, Michaels L, Ullah N *et al.* Adverse events associated with anticoagulation therapy in the periendoscopic period. *Gastrointest. Endosc.* 2010; **71**: 1211–7.

33 Choudari CP, Rajgopal C, Palmer KR. Acute gastrointestinal haemorrhage in anticoagulated patients: Diagnoses and response to endoscopic treatment. *Gut* 1994; **35**: 464–6.

34 Yamamoto T, Kuyama Y, Kozuma K *et al.* Low-dose aspirin prolongs bleeding after gastric biopsy in Japanese patients. *Thromb. Res.* 2008; **122**: 722–3.

35 Yamamoto T, Kuyama Y, Kozuma K *et al.* Antiplatelet agents and bleeding time after endoscopic biopsy of the gastric antrum in Japanese patients. *Dig. Endosc.* 2010; **22**: 250.

36 Kim JS, Lee KS, Kim YI *et al.* A randomized crossover comparative study of aspirin, cilostazol and clopidogrel in normal controls: Analysis with quantitative bleeding time and platelet aggregation test. *J. Clin. Neurosci.* 2004; **11**: 600–2.

37 Yanagisawa A, Sakata K, Miyagawa M *et al.* Impact of ethyl icosapentate and ticlopidine combination therapy on hemorrhage time and platelet aggregation. *Clin. Rep.* 1992; **26**: 3193–8. (in Japanese.)

38 Mabe K, Hirayama M, Kato M. Withdrawal of anticoagulants and antiplatelet agents during endoscopy. *Gastroenterol. Endosc.* 2010; **52**: 2976–84. (in Japanese.)

39 Li Y, Sha W, Nie Y *et al.* Effect of intragastric pH on control of peptic ulcer bleeding. *J. Gastroenterol. Hepatol.* 2000; **15**: 148–54.

40 Baron TH, Harewood GC. Endoscopic balloon dilation of the biliary sphincter compared to endoscopic biliary sphincterotomy for removal of common bile duct stones during ERCP: A metaanalysis of randomized, controlled trials. *Am. J. Gastroenterol.* 2004; **99**: 1455–60.

41 Hussain N, Alsulaiman R, Burtin P *et al.* The safety of endoscopic sphincterotomy in patients receiving antiplatelet agents: A case-control study. *Aliment. Pharmacol. Ther.* 2007; **25**: 579–84.

42 Mannen K, Tsunada S, Hara M *et al.* Risk factors for complications of endoscopic submucosal dissection in gastric tumors: Analysis of 478 lesions. *J. Gastroenterol.* 2010; **45**: 30–6.

43 Okada K, Yamamoto Y, Kasuga A *et al.* Risk factors for delayed bleeding after endoscopic submucosal dissection for gastric neoplasm. *Surg. Endosc.* 2011; **25**: 98–107.

44 Ono S, Fujishiro M, Niimi K *et al.* Technical feasibility of endoscopic submucosal dissection for early gastric cancer in patients taking anti-coagulants or antiplatelet agents. *Dig. Liver Dis.* 2009; **41**: 725–8.

45 Tsuji Y, Ohata K, Ito T *et al.* Risk factors for bleeding after endoscopic submucosal dissection for gastric lesions. *World J. Gastroenterol.* 2010; **16**: 2913–7.

46 Metz AJ, Bourke MJ, Moss A *et al.* Factors that predict bleeding following endoscopic mucosal resection of large colonic lesions. *Endoscopy* 2011; **43**: 506–11.

47 Tounou S, Morita Y. Risks associated with gastric and duodenal ESD under ongoing low dose aspirin therapy. *Gastroenterol. Endosc.* 2010; **53**: 3326–35. (in Japanese.)

48 Singh M, Mehta N, Murthy UK *et al.* Postpolypectomy bleeding in patients undergoing colonoscopy on uninterrupted clopidogrel therapy. *Gastrointest. Endosc.* 2010; **71**: 998–1005.

49 Uchiyama S, Demaerschalk BM, Goto S *et al.* Stroke prevention by cilostazol in patients with atherothrombosis: Meta-analysis of placebo-controlled randomized trials. *J. Stroke Cerebrovasc. Dis.* 2009; **18**: 482–90.

50 White RH, McKittrick T, Hutchinson R *et al.* Temporary discontinuation of warfarin therapy: Changes in the international normalized ratio. *Ann. Intern. Med.* 1995; **1**: 40–2.

51 Tsuji H. Clinical thrombosis and hemostasis techniques for interns III: Appropriate use of heparin formulations. *J. Thromb. Haemost.* 2008; **19**: 187–90. (in Japanese.)

52 Hirsh J, Warkentin TE, Shaughnessy SG *et al.* Heparin and low-molecular-weight heparin: Mechanisms of action, pharmacokinetics, dosing, monitoring, efficacy, and safety. *Chest* 2001; **119** (1 Suppl): 64S–94S.

53 Harrison L, Johnston M, Massicotte MP *et al.* Comparison of 5-mg and 10-mg loading doses in initiation of warfarin therapy. *Ann. Intern. Med.* 1997; **15**: 133–6.

54 Atrial Fibrillation Investigators. Risk factors for stroke and efficacy of antithrombotic therapy in atrial fibrillation. Analysis of pooled data from five randomized controlled trials. *Arch. Intern. Med.* 1994; **154**: 1449–57.

55 The European Atrial Fibrillation Trial Study Group. The optimal anticoagulation therapy in patients with non-rheumatic atrial fibrillation and recent cerebral ischemia. *N. Engl. J. Med.* 1995; **333**: 5–10.

56 Guerrouij M, Uppal CS, Alklabi A *et al.* The clinical impact of bleeding during oral anticoagulant therapy: Assessment of morbidity, mortality and post-bleed anticoagulant management. *J. Thromb. Thrombolysis* 2011; **31**: 419–23.

57 Hui AJ, Wong RM, Ching JY *et al.* Risk of colonoscopic polypectomy bleeding with anticoagulants and antiplatelet agents: Analysis of 1657 cases. *Gastrointest. Endosc.* 2004; **59**: 44–8.

58 Witt DM, Delate T, McCool KH *et al.* Incidence and predictors of bleeding or thrombosis after polypectomy in patients receiving and not receiving anticoagulation therapy. *J. Thromb. Haemost.* 2009; **7**: 1982–9.

59 Garcia DA, Regan S, Henault LE *et al.* Risk of thromboembolism with short-term interruption of warfarin therapy. *Arch. Intern. Med.* 2008; **14**: 63–9.

60 Yasaka M, Minematsu K, Yamaguchi T. Optimal intensity of international normalized ratio in warfarin therapy for secondary prevention of stroke in patients with non-valvular atrial fibrillation. *Intern. Med.* 2001; **40**: 1183–8.

61 Constans M, Santamaria A, Mateo J *et al.* Low-molecular-weight heparin as bridging therapy during interruption of oral anticoagulation in patients undergoing colonoscopy or gastroscopy. *Int. J. Clin. Pract.* 2007; **61**: 212–7.

62 Connolly SJ, Ezekowitz MD, Yusuf S *et al.* Dabigatran versus warfarin in patients with atrial fibrillation. *N. Engl. J. Med.* 2009; **361**: 1139–51.

63 Stangier J, Eriksson BI, Dahl OE *et al.* Pharmacokinetic profile of the oral direct thrombin inhibitor dabigatran etexilate in

healthy volunteers and patients undergoing total hip replacement. *J. Clin. Pharmacol.* 2005; **45**: 555–63.
64 Eikelboom JW, Wallentin L, Connolly SJ *et al.* Risk of bleeding with 2 doses of dabigatran compared with warfarin in older and younger patients with atrial fibrillation: An analysis of the randomized evaluation of long-term anticoagulant therapy (RE-LY) trial. *Circulation* 2011; **123**: 2363–72.
65 Watabe H, Yamaji Y, Okamoto M *et al.* Risk assessment for delayed hemorrhagic complication of colonic polypectomy: Polyp-related factors and patient-related factors. *Gastrointest. Endosc.* 2006; **64**: 73–8.
66 Goto O, Fujishiro M, Kodashima S *et al.* A second-look endoscopy after endoscopic submucosal dissection for gastric epithelial neoplasm may be unnecessary: A retrospective analysis of postendoscopic submucosal dissection bleeding. *Gastrointest. Endosc.* 2010; **71**: 241–8.
67 Fujimoto K, Fujishiro M, Kato M *et al.* Guidelines for gastroenterological endoscopy in patients undergoing antithrombotic treatment. *Gastroenterol. Endosc.* 2012; **54**: 2075–102. (in Japanese.)

Nakachi et al. Cancer Imaging 2014, 14:7
http://www.cancerimagingjournal.com/content/14/1/7

Cancer Imaging

RESEARCH ARTICLE Open Access

Prediction of poorly differentiated hepatocellular carcinoma using contrast computed tomography

Kenichiro Nakachi, Hideyuki Tamai*, Yoshiyuki Mori, Naoki Shingaki, Kosaku Moribata, Hisanobu Deguchi, Kazuki Ueda, Izumi Inoue, Takao Maekita, Mikitaka Iguchi, Jun Kato and Masao Ichinose

Abstract

Background: Percutaneous radiofrequency ablation (RFA) is a well-established local treatment for small hepatocellular carcinoma (HCC). However, poor differentiation is a risk factor for tumor seeding or intrahepatic dissemination after RFA for HCC. The present study aimed to develop a method for predicting poorly differentiated HCC using contrast computed tomography (CT) for safe and effective RFA.

Methods: Of HCCs diagnosed histologically, 223 patients with 226 HCCs showing tumor enhancement on contrast CT were analyzed. The tumor enhancement pattern was classified into two categories, with and without non-enhanced areas, and tumor stain that disappeared during the venous or equilibrium phase with the tumor becoming hypodense was categorized as positive for washout.

Results: The 226 HCCs were evaluated as well differentiated (w-) in 56, moderately differentiated (m-) in 137, and poorly differentiated (p-) in 33. The proportions of small HCCs (3 cm or less) in w-HCCs, m-HCCs, and p-HCCs were 86% (48/56), 59% (81/137), and 48% (16/33), respectively. The percentage with heterogeneous enhancement in all HCCs was 13% in w-HCCs, 29% in m-HCCs, and 85% in p-HCCs. The percentage with tumor stain washout in the venous phase was 29% in w-HCCs, 63% in m-HCCs, and 94% in p-HCCs. The percentage with heterogeneous enhancement in small HCCs was 10% in w-HCCs, 10% in m-HCCs, and 75% in p-HCCs. The percentage with tumor stain washout in the venous phase in small HCCs was 23% in w-HCCs, 58% in m-HCCs, and 100% in p-HCCs. Significant correlations were seen for each factor ($p < 0.001$ each). Sensitivity, specificity, positive predictive value, negative predictive value, and accuracy for prediction of poor differentiation in small HCCs by tumor enhancement with non-enhanced areas were 75%, 90%, 48%, 97%, and 88%, respectively; for tumor stain washout in the venous phase, these were 100%, 55%, 22%, 100%, and 60%, respectively.

Conclusions: Tumor enhancement patterns were associated with poor histological differentiation even in small HCCs. Tumor enhancement with non-enhanced areas was valuable for predicting poorly differentiated HCC.

Keywords: Contrast computed tomography, Histological differentiation, Poorly differentiated hepatocellular carcinoma

Background

Percutaneous radiofrequency ablation (RFA) is a well-established local treatment for unresectable small hepatocellular carcinoma (HCC), which is a repeatable and safe procedure. Currently, RFA is considered the standard of care for patients with Barcelona-Clinic Liver Cancer (BCLC) 0-A tumors not suitable for surgery [1]. Recently, Forner et al. [2] proposed RFA instead of resection in patients with very early (<2 cm) HCC.

However, several investigators have reported the risk of seeding [3-5], intrahepatic dissemination [6,7], and aggressive recurrence after RFA [8-10]. Some investigators reported that these critical recurrences were related to poor differentiation [4,7]. Therefore, poor differentiation would be a risk factor for tumor seeding or intrahepatic dissemination after RFA for HCC. Furthermore, the prognosis of patients with poorly differentiated HCCs is worse even with radical therapy [11-13]. Along with de-differentiation from well to moderately/poorly differentiated HCC, even small HCCs have a greater tendency for vascular invasion and intrahepatic metastasis

* Correspondence: tamahide@wakayama-med.ac.jp
Second Department of Internal Medicine, Wakayama Medical University, 811-1 Kimiidera, Wakayama 641-0012, Japan

[14,15]. Fukuda et al. [16] recommended that, when hepatic function is well preserved, hepatic resection should be the first choice for local control, especially in cases of moderately to poorly differentiated HCC. Therefore, the prediction of poorly differentiated HCC before therapy is crucial for deciding the optimal therapeutic strategy and for safe and effective RFA even for small HCCs.

Contrast computed tomography (CT) is commonly used for definite diagnosis of HCCs on imaging [17]. However, the differential diagnosis of poorly differentiated HCC using contrast CT has not been sufficiently established. In the present study, correlations between the enhancement pattern on contrast CT and histological differentiation, and the ability to predict poorly differentiated HCC using contrast CT were analyzed.

Results

Correlation of tumor size and histological differentiation

The histological classification was w-HCC in 56, m-HCC in 137, and p-HCC in 33. Mean diameter by histological classification was 26 ± 13 mm in w-HCCs, 33 ± 20 mm in m-HCCs, and 44 ± 33 mm in p-HCCs. The tumor size was significantly larger as the histological differentiation grade advanced ($p = 0.03$). In pairwise comparisons, tumor size was significantly smaller for w-HCCs than for m-HCCs and p-HCCs ($P = 0.003$ and $p = 0.001$). However, there was no significant difference between m-HCCs and p-HCCs ($p = 1.000$). The proportions of small HCCs (3 cm or less) in w-HCCs, m-HCCs, and p-HCCs were 86% (48/56), 59% (81/137), and 48% (16/33), respectively. The proportions of w-HCCs, m-HCCs, and p-HCCs in small HCCs were 33% (48/145), 56% (81/145), and 11% (16/145), respectively.

Correlation between tumor enhancement patterns and histological differentiation

The correlation between tumor enhancement patterns in the arterial phase and histological differentiation is shown in Table 1. The percentage of tumors with tumor stain with non-enhanced areas was significantly higher as the histological differentiation grade advanced ($p < 0.001$). In pairwise comparisons, there was a significant difference between m-HCCs and p-HCCs. However, there was no significant difference between w-HCCs and m-HCCs. As in all HCCs, there was also a significant correlation even in small HCCs (3 cm or less in diameter).

Correlation between tumor stain washout and histological differentiation

The correlation between tumor stain washout in the venous phase and histological differentiation is shown in Table 2. The percentage of tumors with tumor stain washout in the venous phase was significantly higher as the histological differentiation grade advanced ($p < 0.001$). In pairwise comparisons, there were significant differences among all groups ($p < 0.05$). As in all HCCs, there were also significant correlations even in small HCCs.

Table 1 Correlation between tumor enhancement pattern in the arterial phase and histological differentiation

Tumor enhancement in the arterial phase	Histological differentiation			
	Well	Moderately	Poorly	p-value
All HCCs	n = 56	n = 137	n = 33	
With non-enhanced areas (n = 74)	7 (13%)	39 (29%)	28 (85%)	
Without non-enhanced areas (n = 152)	49 (88%)	98 (72%)	5 (15%)	<0.001
Small HCCs (3 cm or less)	n = 48	n = 81	n = 16	
With non-enhanced areas (n = 25)	5 (10%)	8 (10%)	12 (75%)	
Without non-enhanced areas (n = 120)	43 (90%)	73 (90%)	4 (25%)	<0.001

HCC, hepatocellular carcinoma.
The p-value was calculated among each differentiation group by with versus without non-enhanced area using Fisher's exact test.

The correlation between tumor stain washout in the equilibrium phase and histological differentiation is shown in Table 3. The percentage of tumors with tumor stain washout in the equilibrium phase was higher as the histological differentiation grade advanced ($p < 0.001$). However, in comparisons of each pair, no significant difference was observed between m-HCCs and p-HCCs. As in all HCCs, there were also significant correlations even in small HCCs between tumor stain washout in the equilibrium phase and histological differentiation.

Sensitivity, specificity, positive predictive value, negative predictive value, and accuracy for the prediction of poorly differentiated HCC

Sensitivity, specificity, PPV, NPV, and accuracy for the prediction of p-HCC by each CT finding are shown in Table 4. Sensitivity for p-HCC was inferior by tumor enhancement with non-enhanced areas than by tumor stain washout in the venous phase. However, specificity and accuracy for p-HCC were superior by tumor enhancement with non-enhanced areas than by tumor stain washout in the venous phase. These findings were seen even in small HCCs. Although accuracies for p-HCC in both all HCCs and small HCCs were slightly improved by the combination of tumor enhancement with non-enhanced areas and tumor stain washout in the venous phase, these improvements were not significant.

Discussion

With respect to a hemodynamic change from m-HCC to p-HCC, Asayama et al. [18] reported that the arterial blood supply decreases significantly. Furthermore, it was also found that, although hypervascular tumor was predominant in p-HCCs, the proportion of hypovascular tumors

Table 2 Correlation between tumor stain washout in the venous phase and histological differentiation

Tumor stain washout in the venous phase	Histological differentiation			
	Well	Moderately	Poorly	p-value
All HCCs	n = 56	n = 137	n = 33	
Positive (n = 133)	16 (29%)	86 (63%)	31 (94%)	
Negative (n = 93)	40 (71%)	51 (37%)	2 (6%)	<0.001
Small HCCs (3 cm or less)	n = 48	n = 81	n = 16	
Positive (n = 74)	11 (23%)	47 (58%)	16 (100%)	
Negative (n = 71)	37 (77%)	34 (42%)	0 (0%)	<0.001

HCC, hepatocellular carcinoma.
The p-value was calculated among each differentiation group by positive versus negative tumor stain washout using Fisher's exact test.

was higher in w-HCCs and p-HCCs than in m-HCCs on contrast ultrasonography [19] and contrast CT [20]. However, Jang et al. [19] indicated that there was no significant difference in arterial vascularity between w-HCCs and p-HCCs on contrast ultrasonography. Lee et al. [20] also demonstrated that no significant difference was seen in the prevalence of atypical arterial enhancement such as hypoattenuation between w-HCCs and p-HCCs on contrast CT. These studies did not analyze the diagnostic values for p-HCC using arterial hypovascularity. Sanda et al. [21] demonstrated that even small HCCs (diameter up to 2 cm) intermingled with hypovascular areas and hypervascular areas on the arterial phase of contrast CT showed contiguous multinodular type and included p-HCC components. Kawamura et al. [22] reported that heterogeneous enhancement with irregular ring-like structures in the arterial phase of contrast CT is a significant independent predictor of p-HCC. Of course, their heterogeneous enhancement pattern with irregular ring-like structures was included in the criteria of tumor enhancement with non-enhanced areas in the present study. From the above, it is assumed that a hemodynamic change from hypervascularity to hypovascularity in overt HCC means that p-HCC components have been generated in the HCC. Accordingly, the present arterial tumor enhancement classification with or without non-enhanced areas is reasonable for predicting hypervascular HCC including p-HCC components.

Table 3 Correlation between tumor stain washout in the equilibrium phase and histological differentiation

Tumor stain washout in the equilibrium phase	Histological differentiation			
	Well	Moderately	Poorly	p-value
All HCCs	n = 56	n = 137	n = 33	
Positive (n = 197)	39 (70%)	125 (91%)	33 (100%)	
Negative (n = 29)	17 (30%)	12 (9%)	0 (0%)	<0.001
Small HCCs (3 cm or less)	n = 48	n = 81	n = 16	
Positive (n = 118)	32 (67%)	70 (86%)	16 (100%)	
Negative (n = 27)	16 (33%)	11 (14%)	0 (0%)	0.003

HCC, hepatocellular carcinoma.
The p-value was calculated among each differentiation group by positive versus negative tumor stain washout using Fisher's exact test.

With respect to other enhancement pattern findings of contrast CT associated with p-HCC, tumor stain washout in the venous phase has been reported. Nishie et al. [23] indicated that p-HCCs are considered to show faster tumor stain washout on contrast CT than non-p-HCCs. On contrast magnetic resonance imaging, it has also been reported that tumor stain washout in the venous phase was more frequently seen in p-HCCs [24,25]. Furthermore, on contrast-enhanced ultrasonography, tumor stain washout time was significantly less in p-HCCs [19,26]. From the various above contrast studies and the present results, there is no doubt that tumor stain washout becomes faster as the histological differentiation of HCC advances.

In the present study, the diagnostic accuracy for p-HCC using tumor enhancement with non-enhanced areas in the arterial phase of contrast CT was high even in small HCCs. On the other hand, the accuracy for p-HCC by tumor stain washout in the venous phase of contrast CT was not as high. In the present results, tumor enhancement with non-enhanced areas and tumor stain washout in the venous phase were associated with poor histological differentiation even in small HCCs. However, the improvement of accuracies for p-HCC in both all HCCs and small HCCs by the combination of tumor enhancement with non-enhanced areas and tumor stain washout in the venous phase were slight, and these improvements were not significant. Therefore, tumor enhancement with non-enhanced areas appears to be the most valuable finding on contrast CT in the prediction of poorly differentiated HCC.

The present study had some limitations. First, the present study was retrospective. Furthermore, HCCs with no enhancement in the arterial phase of contrast CT were not evaluated. Therefore, the present results cannot be generalized to HCCs without arterial enhancement on contrast CT. Second, needle biopsy samples were used. The assessment of histological differentiation grade using biopsy samples may not reflect the lowest differentiated component in the tumor. Nevertheless, the present results could suggest that the contrast CT enhancement pattern facilitates assessment of histological malignant potential. Third, this study could not show the correlation between the contrast CT enhancement pattern and the prognosis. Kawamura et al. [27] reported that a heterogeneous enhancement pattern with irregular ringed-like structures on dynamic CT is associated with tumor recurrence after RFA. However, their study was very small. In the future, a large-scale cohort study should be conducted to investigate whether these findings will contribute to predicting outcome after RFA.

Table 4 Sensitivity, specificity, positive predictive value, negative predictive value, and accuracy of prediction for poorly differentiated hepatocellular carcinoma using CT findings

CT findings	Sensitivity	Specificity	PPV	NPV	Accuracy
All HCCs					
Enhancement with non-enhanced area	85%	76%	34%	97%	77%
Tumor stain washout in the venous phase	94%	47%	23%	98%	54%
Both findings positive	79%	80%	40%	96%	80%
Small HCCs (3 cm or less)					
Enhancement with non-enhanced area	75%	90%	48%	97%	88%
Tumor stain washout in the venous phase	100%	55%	22%	100%	60%
Both findings positive	75%	92%	55%	97%	90%

CT, computed tomography; PPV, positive predictive value; NPV, negative predictive value; HCC, hepatocellular carcinoma.

Conclusions

In conclusion, arterial tumor enhancement with non-enhanced areas and tumor stain washout in the venous phase were associated with poor histological differentiation even in small HCCs, and tumor enhancement with non-enhanced areas was the most valuable finding in the prediction of poorly differentiated HCC. For safe and effective RFA for small HCCs, systematic resection should be considered as the treatment of first choice for small HCCs with arterial tumor enhancement with non-enhanced areas, because the prevalence of microscopic vascular invasion or intrahepatic metastasis is quite high in p-HCCs. If unresectable, combinations of RFA with transcatheter arterial chemo-embolization should be considered as alternative treatment strategies. However, further study and analysis are required to determine whether this approach actually helps improve the prognosis of small p-HCCs.

Table 5 Patients' characteristics

Age (years; mean ± SD)	68.3 ± 8.2
Sex (male/female)	147/76
Etiology (HCV/non-HCV)	172/51
Tumor size (mm; mean ± SD)	33 ± 22
Number of tumors (mean ± SD)	1.7 ± 1.2
AFP (ng/mL; mean ± SD)	3026.6 ± 35190.2
AFP-L3 (%; mean ± SD)	14.5 ± 24.7
DCP (mAU/mL; mean ± SD)	4130.0 ± 23805.1
Child class (A/B/C)	161/55/7
Activity stage (A0/1/2/3)	11/99/98/15
Fibrosis grade (F0/1/2/3/4)	7/21/39/68/88

SD, standard deviation; HCV, hepatitis C virus; AFP, alpha-fetoprotein; AFP-L3, lens culinaris agglutinin-reactive alpha-fetoprotein; DCP, Des-gamma-carboxyprothrombin.

Methods

Patients

In our hospital's HCC database, 310 patients with 315 HCC nodules were histologically diagnosed by tumor biopsy or surgical resection between May 2001 and December 2010. The flowchart of patient enrollment is shown in Figure 1. Of 226 HCC nodules, 165 were diagnosed by tumor biopsy, and 61 were diagnosed by resection. The patients' characteristics are summarized in Table 5. This retrospective study was approved by our ethics committee and conformed to the Helsinki Declaration. The need for patients to give written, informed consent was waived by our ethics committee.

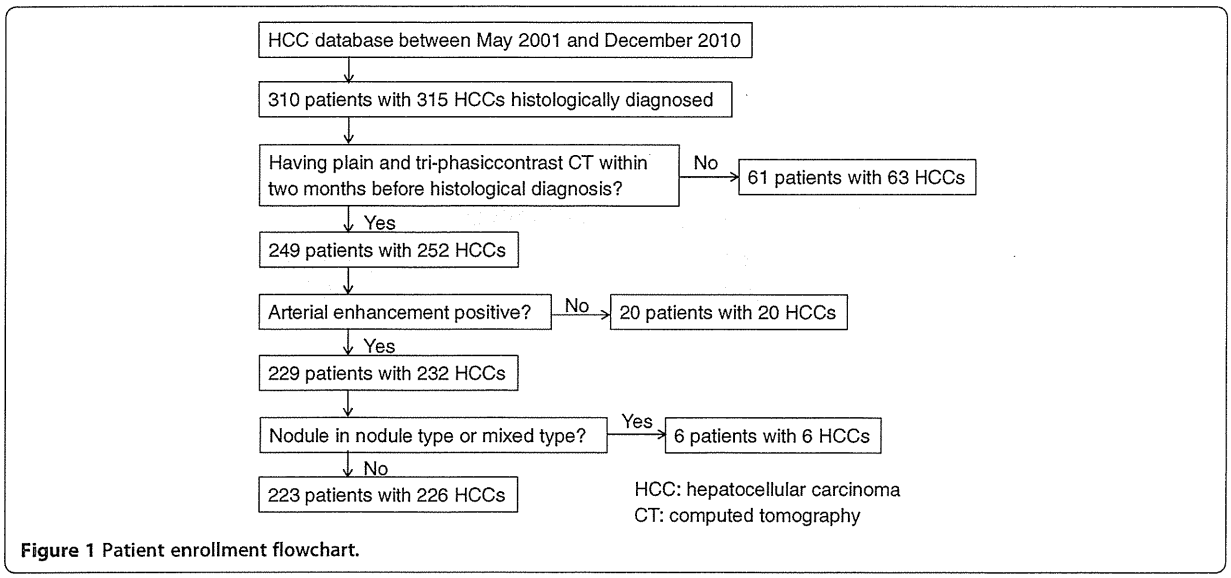

Figure 1 Patient enrollment flowchart.

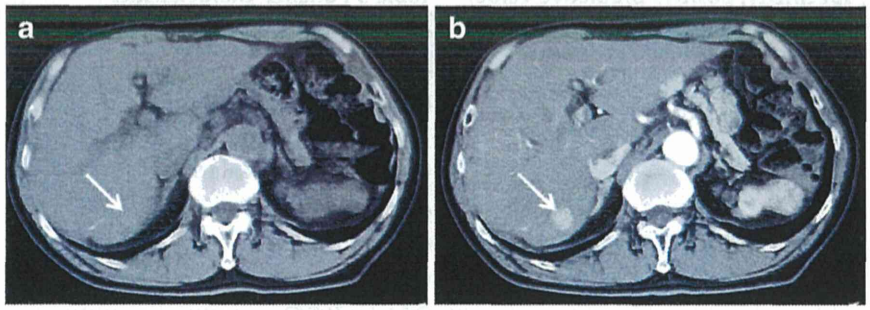

Figure 2 Tumor enhancement without non-enhanced areas. The pre-contrast image **(a)** shows an iso-density tumor. In comparison with pre-contrast image, the tumor stain has no non-enhanced areas in the arterial phase **(b)**. The tumor is indicated by arrows.

Technique and analysis

All contrast CT examinations were performed with multi-detector row CT scanners having at least 4 detectors (Aquilion, Toshiba Medical Systems, Tochigi, Japan or Light speed VCT, GE Medical Systems, Milwaukee, WI, USA) with a section thickness of 5 mm. In addition to plain images, arterial phase images were obtained 40 seconds after the start of bolus administration. From 2005 onward, the arterial phase was scanned with an automatic bolus-tracking program. Venous and equilibrium phase images were obtained at 70 seconds and 180 seconds, respectively. All patients received a non-ionic iodinated contrast medium at a dose of 580 mgI/kg; it was administered to all patients by an automated power injector for 30 seconds (19.3 mgI/kg/s).

Contrast CT findings related to tumor enhancement pattern and washout were categorized as follows. Tumor enhancement pattern in the arterial phase was classified into two categories, with and without non-enhanced areas (Figures 2 and 3). Tumor stain obtained during the arterial phase that disappeared during the venous or equilibrium phase, with the tumor becoming hypodense, was categorized as positive for washout. Images obtained by contrast CT were independently analyzed using the above criteria of enhancement patterns without reference to histological differentiation by two experienced readers with more than 20 years of experience in liver imaging. Any disagreements in interpretation were resolved by consensus.

Needle biopsies of tumors were performed using an 18-gauge needle (Bard Monopty® C.R. Bard Inc., Covington, GA, USA). Liver biopsy was performed using a 16-gauge needle. Histological findings were classified using the METAVIR scoring system [28]. All biopsy and resected specimens were examined by two experienced pathologists, without reference to the CT findings of their tumors and surrounding livers. According to the International Working Party classification [29], HCC histology was classified into three types: well differentiated (w-), moderately differentiated (m-), and poorly differentiated (p-) HCCs. If heterogeneous differentiation was found in the obtained HCC tissue, differentiation grade was classified based on the lowest differentiated grade. Any discrepancies between the two pathologists with more than 20 years of experience in liver pathology were resolved by discussion to reach consensus.

Statistical analysis

Values are expressed as means ± standard deviation (SD). The correlation between tumor size and histological differentiation was analyzed using the Jonckheere-Terpstra test. The correlation between the enhancement pattern and histological differentiation was analyzed using Fisher's exact test or the chi-square test of independence.

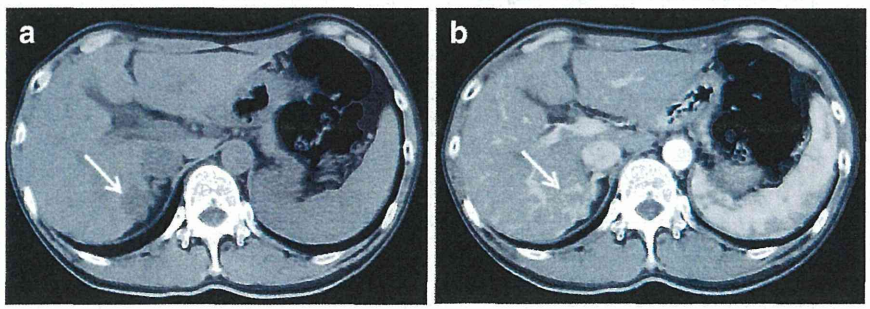

Figure 3 Tumor enhancement with non-enhanced areas. The pre-contrast image **(a)** shows a low-density tumor. In comparison with the pre-contrast image, the tumor stain has non-enhanced areas in the arterial phase **(b)**. The tumor is indicated by arrows.

Sensitivity, specificity, positive predictive value (PPV), negative predictive value (NPV), and accuracy for diagnosis of p-HCC were calculated according to findings on contrast CT. Accuracy between groups was compared using the McNemar test. A p value less than 0.05 was considered significant. All analyses were performed using the SPSS 20.0 software package (SPSS, Inc., Chicago, IL, USA).

Abbreviations

HCC: Hepatocellular carcinoma; RFA: Percutaneous radiofrequency ablation; CT: Computed tomography; BCLC: Barcelona-clinic liver cancer; w: Well differentiated; m: Moderately differentiated; p: Poorly differentiated; SD: Standard deviation; PPV: positive predictive value; NPV: Negative predictive value.

Competing interests

The authors declare that they have no competing interests.

Authors' contributions

NK, TH and IM designed and proposed the research; all authors approved the analysis and participated in drafting the article; MY, SN, MK, DH, UK, II, MT, IM, and KJ collected the clinical data; TH and IM analyzed imaging examinations; NK and TH performed the statistical analysis; NK and TH wrote the manuscript. All authors read and approved the final manuscript.

Received: 3 November 2013 Accepted: 27 January 2014
Published: 22 April 2014

References

1. European Association For The Study Of The Liver, European Organisation For Research and Treatment Of Cancer: **EASL-EORTC clinical practice guidelines: management of hepatocellular carcinoma.** *J Hepatol* 2012, **56**:908–943.
2. Forner A, Llovet JM, Bruix J: **Hepatocellular carcinoma.** *Lancet* 2012, **379**:1245–1255.
3. Llovet JM, Vilana R, Bru C, Bianchi L, Salmeron JM, Boix L, Ganau S, Sala M, Pages M, Ayuso C, Sole M, Rodes J, Bruix J: **Increased risk of tumor seeding after percutaneous radiofrequency ablation for single hepatocellular carcinoma.** *Hepatol* 2001, **33**:1124–1129.
4. Imamura J, Tateishi R, Shiina S, Goto E, Sato T, Ohki T, Masuzaki R, Goto T, Yoshida H, Kanai F, Hamamura K, Obi S, Omata M: **Neoplastic seeding after radiofrequency ablation for hepatocellular carcinoma.** *Am J Gastroenterol* 2008, **103**:3057–3062.
5. Shirai K, Tamai H, Shingaki N, Mori Y, Moribata K, Enomoto S, Deguchi H, Ueda K, Maekita T, Inoue I, Iguchi M, Yanaoka K, Oka M, Ichinose M: **Clinical features and risk factors of extrahepatic seeding after percutaneous radiofrequency ablation for hepatocellular carcinoma.** *Hepatol Res* 2011, **41**:738–745.
6. Nicoli N, Casaril A, Hilal MA, Mangiante G, Marchiori L, Ciola M, Invernizzi L, Campagnaro T, Mansueto G: **A case of rapid intrahepatic dissemination of hepatocellular carcinoma after radiofrequency thermal ablation.** *Am J Surg* 2004, **188**:165–167.
7. Mori Y, Tamai H, Shingaki N, Moribata K, Shiraki T, Deguchi H, Ueda K, Enomoto S, Magari H, Inoue I, Maekita T, Iguchi M, Yanaoka K, Oka M, Ichinose M: **Diffuse intrahepatic recurrence after percutaneous radiofrequency ablation for solitary and small hepatocellular carcinoma.** *Hepatol Int* 2009, **3**:509–515.
8. Seki T, Tamai T, Ikeda K, Imamura M, Nishimura A, Yamashiki N, Nakagawa T, Inoue K: **Rapid progression of hepatocellular carcinoma after transcatheter arterial chemoembolization and percutaneous radiofrequency ablation in the primary tumour region.** *Eur J Gastroenterol Hepatol* 2001, **13**:291–294.
9. Takada Y, Kurata M, Ohkohchi N: **Rapid and aggressive recurrence accompanied by portal tumor thrombus after radiofrequency ablation for hepatocellular carcinoma.** *Int J Clin Oncol* 2003, **8**:332–335.
10. Ruzzenente A, Manzoni GD, Molfetta M, Pachera S, Genco B, Donataccio M, Guglielmi A: **Rapid progression of hepatocellular carcinoma after radiofrequency ablation.** *World J Gastroenterol* 2004, **10**:1137–1140.
11. Sasaki Y, Imaoka S, Ishiguro S, Nakano H, Kasugai H, Fujita M, Inoue E, Ishikawa O, Furukawa H, Nakamori S, Kuroda C, Iwanaga T: **Clinical features of small hepatocellular carcinomas as assessed by histologic grades.** *Surgery* 1996, **119**:252–260.
12. Oishi K, Itamoto T, Amano H, Fukuda S, Ohdan H, Tashiro H, Shimamoto F, Asahara T: **Clinicopathologic features of poorly differentiated hepatocellular carcinoma.** *J Surg Oncol* 2007, **95**:311–316.
13. Kim SH, Lim HK, Choi D, Lee WJ, Kim MJ, Kim CK, Jeon YH, Lee JM, Rhim H: **Percutaneous radiofrequency ablation of hepatocellular carcinoma: effect of histologic grade on therapeutic results.** *AJR Am J Roentgenol* 2006, **186**:S327–S333.
14. Esnaola NF, Lauwers GY, Mirza NQ, Nagorney DM, Doherty D, Ikai I, Yamaoka Y, Regimbeau JM, Belghiti J, Curley SA, Ellis LM, Vauthey JN: **Predictors of microvascular invasion in patients with hepatocellular carcinoma who are candidates for orthotopic liver transplantation.** *J Gastrointest Surg* 2002, **6**:224–232. discussion 232.
15. Nakashima Y, Nakashima O, Tanaka M, Okuda K, Nakashima M, Kojiro M: **Portal vein invasion and intrahepatic micrometastasis in small hepatocellular carcinoma by gross type.** *Hepatol Res* 2003, **26**:142–147.
16. Fukuda S, Itamoto T, Nakahara H, Kohashi T, Ohdan H, Hino H, Ochi M, Tashiro H, Asahara T: **Clinicopathologic features and prognostic factors of resected solitary small-sized hepatocellular carcinoma.** *Hepatogastroenterology* 2005, **52**:1163–1167.
17. **Clinical practice guidelines for hepatocellular carcinoma - the Japan society of hepatology 2009 update.** *Hepatol Res* 2010, **40**(Suppl 1):2–144.
18. Asayama Y, Yoshimitsu K, Nishihara Y, Irie H, Aishima S, Taketomi A, Honda H: **Arterial blood supply of hepatocellular carcinoma and histologic grading: radiologic-pathologic correlation.** *AJR Am J Roentgenol* 2008, **190**:W28–W34.
19. Jang HJ, Kim TK, Burns PN, Wilson SR: **Enhancement patterns of hepatocellular carcinoma at contrast-enhanced US: comparison with histologic differentiation.** *Radiology* 2007, **244**:898–906.
20. Lee JH, Lee JM, Kim SJ, Baek JH, Yun SH, Kim KW, Han JK, Choi BI: **Enhancement patterns of hepatocellular carcinomas on multiphasic multidetector row CT: comparison with pathological differentiation.** *Br J Radiol* 2012, **85**:e573–e583.
21. Sanada Y, Yoshida K, Itoh H: **Comparison of CT enhancement patterns and histologic features in hepatocellular carcinoma up to 2 cm: assessment of malignant potential with claudin-10 immunohistochemistry.** *Oncol Rep* 2007, **17**:1177–1182.
22. Kawamura Y, Ikeda K, Hirakawa M, Yatsuji H, Sezaki H, Hosaka T, Akuta N, Kobayashi M, Saitoh S, Suzuki F, Suzuki Y, Arase Y, Kumada H: **New classification of dynamic computed tomography images predictive of malignant characteristics of hepatocellular carcinoma.** *Hepatol Res* 2010, **40**:1006–1014.
23. Nishie A, Yoshimitsu K, Okamoto D, Tajima T, Asayama Y, Ishigami K, Kakihara D, Nakayama T, Takayama Y, Shirabe K, Fujita N, Honda H: **CT prediction of histological grade of hypervascular hepatocellular carcinoma: utility of the portal phase.** *Jpn J Radiol* 2013, **31**:89–98.
24. Enomoto S, Tamai H, Shingaki N, Mori Y, Moribata K, Shiraki T, Deguchi H, Ueda K, Inoue I, Maekita T, Iguchi M, Yanaoka K, Oka M, Ichinose M: **Assessment of hepatocellular carcinomas using conventional magnetic resonance imaging correlated with histological differentiation and a serum marker of poor prognosis.** *Hepatol Int* 2011, **5**:730–737.
25. Okamoto D, Yoshimitsu K, Nishie A, Tajima T, Asayama Y, Ishigami K, Hirakawa M, Ushijima Y, Kakihara D, Nakayama T, Nishihara Y, Aishima S, Taketomi A, Kishimoto J, Honda H: **Enhancement pattern analysis of hypervascular hepatocellular carcinoma on dynamic MR imaging with histopathological correlation: validity of portal phase imaging for predicting tumor grade.** *Eur J Radiol* 2012, **81**:1116–1121.
26. Fan ZH, Chen MH, Dai Y, Wang YB, Yan K, Wu W, Yang W, Yin SS: **Evaluation of primary malignancies of the liver using contrast-enhanced sonography: correlation with pathology.** *AJR Am J Roentgenol* 2006, **186**:1512–1519.
27. Kawamura Y, Ikeda K, Seko Y, Hosaka T, Kobayashi M, Saitoh S, Kumada H: **Heterogeneous type 4 enhancement of hepatocellular carcinoma on dynamic CT is associated with tumor recurrence after radiofrequency ablation.** *AJR Am J Roentgenol* 2011, **197**:W665–W673.
28. Bedossa P, Poynard T: **An algorithm for the grading of activity in chronic hepatitis C. The METAVIR Cooperative Study Group.** *Hepatol* 1996, **24**:289–293.
29. **Terminology of nodular hepatocellular lesions. International working party.** *Hepatol* 1995, **22**:983–993.

doi:10.1186/1470-7330-14-7
Cite this article as: Nakachi *et al.*: Prediction of poorly differentiated hepatocellular carcinoma using contrast computed tomography. *Cancer Imaging* 2014 **14**:7.

OPEN ACCESS Freely available online

PLOS | ONE

Gli Regulates *MUC5AC* Transcription in Human Gastrointestinal Cells

Natsuko Kageyama-Yahara[1☯], Nobutake Yamamichi[1*☯], Yu Takahashi[1], Chiemi Nakayama[1], Kazuya Shiogama[2], Ken-ichi Inada[2], Maki Konno-Shimizu[1], Shinya Kodashima[1], Mitsuhiro Fujishiro[1], Yutaka Tsutsumi[2], Masao Ichinose[3], Kazuhiko Koike[1]

1 Department of Gastroenterology, Graduate School of Medicine, The University of Tokyo, Bunkyo-ku, Tokyo, Japan, **2** 1st Department of Pathology, Fujita Health University School of Medicine, Toyoake, Aichi, Japan, **3** Second Department of Internal Medicine, Wakayama Medical College, Kimiidera, Wakayama, Japan

Abstract

MUC5AC is a well-known gastric differentiation marker, which has been frequently used for the classification of stomach cancer. Immunohistochemistry revealed that expression of MUC5AC decreases accompanied with increased malignant property of gastric mucosa, which further suggests the importance of *MUC5AC* gene regulation. Alignment of the 5′-flanking regions of *MUC5AC* gene of 13 mammal species denoted high homology within 200 bp upstream of the coding region. Luciferase activities of the deletion constructs containing upstream 451 bp or shorter fragments demonstrated that 15 bp region between −111 and −125 bp plays a critical role on *MUC5AC* promoter activity in gastrointestinal cells. We found a putative Gli-binding site in this 15 bp sequence, and named this region a highly conserved region containing a Gli-binding site (HCR-Gli). Overexpression of Gli homologs (Gli1, Gli2, and Gli3) clearly enhanced *MUC5AC* promoter activity. Exogenous modulation of Gli1 and Gli2 also affected the endogenous *MUC5AC* gene expression in gastrointestinal cells. Chromatin immunoprecipitation assays demonstrated that Gli1 directly binds to HCR-Gli: Gli regulates *MUC5AC* transcription via direct protein-DNA interaction. Conversely, in the 30 human cancer cell lines and various normal tissues, expression patterns of MUC5AC and Gli did not coincide wholly: MUC5AC showed cell line-specific or tissue-specific expression whereas Gli mostly revealed ubiquitous expression. Luciferase promoter assays suggested that the far distal *MUC5AC* promoter region containing upstream 4010 bp seems to have several enhancer elements for gene transcription. In addition, treatments with DNA demethylation reagent and/or histone deacetylase inhibitor induced *MUC5AC* expression in several cell lines that were deficient in MUC5AC expression. These results indicated that Gli is necessary but not sufficient for *MUC5AC* expression: namely, the multiple regulatory mechanisms should work in the distal promoter region of *MUC5AC* gene.

Citation: Kageyama-Yahara N, Yamamichi N, Takahashi Y, Nakayama C, Shiogama K, et al. (2014) Gli Regulates *MUC5AC* Transcription in Human Gastrointestinal Cells. PLoS ONE 9(8): e106106. doi:10.1371/journal.pone.0106106

Editor: Arun Rishi, Wayne State University, United States of America

Received June 5, 2014; **Accepted** July 28, 2014; **Published** August 28, 2014

Data Availability: The authors confirm that all data underlying the findings are fully available without restriction. All relevant data are within the paper and its Supporting Information files.

Funding: This work was supported in part by a grant from Takeda Science Foundation, in part by a research grant from the Tokyo Society of Medical Sciences, in part by Grant-in-Aid for Scientific Research (C) from the Japan Society for the Promotion of Science, in part by Sato Memorial Foundation for Cancer Research, in part by a research grant from Nakayama Cancer Research Institute, in part by a research grant from Foundation for promotion of Cancer Research, and also in part by Grant-in-Aid for Young Scientists (B) from the Ministry of Education, Culture, Sports, Science and Technology (MEXT). All the funders had no role in study design, data collection and analysis, decision to publish, or preparation of the manuscript. The URLs and grant numbers are as follows: A grant from Takeda Science Foundation, http://www.takeda-sci.or.jp/assist/, Grant number: N/A (Grant in 2012); a research grant from the Tokyo Society of Medical Sciences, http://square.umin.ac.jp/igakukai/02toppage/toppage.html, Grant number: N/A (Grant in 2012); Grant-in-Aid for Scientific Research (C) from the Japan Society for the Promotion of Science, http://www.jsps.go.jp/english/e-grants/index.html, Grant number: 25460381 (Grant in 2012–2014); Sato Memorial Foundation for Cancer Research, http://www.jca.gr.jp/researcher/reward/2010/sato.html, Grant number: N/A (Grant in 2011); a research grant from Nakayama Cancer Research Institute, http://ncri.or.jp/project/project.html, Grant number: N/A (Grant in 2010); a research grant from Foundation for promotion of Cancer Research, http://www.fpcr.or.jp/about/index.html, Grant number: N/A (Grant in 2010); Grant-in-Aid for Young Scientists (B) from the Ministry of Education, Culture, Sports, Science and Technology (MEXT), http://www.jsps.go.jp/english/e-grants/index.html, Grant number: 23790355 (Grant in 2010–2011).

Competing Interests: The authors have declared that no competing interests exist.

* Email: nyamamic-tky@umin.ac.jp

☯ These authors contributed equally to this work.

Introduction

Although the mortality and incidence of gastric cancer has gradually fallen in the last several decades, it is still the fourth most common malignancy and the second leading cause of cancer-related death worldwide [1]. Gastric cancer mainly occurs from gastric mucosa with intestinal metaplasia, which is mostly caused by chronic infection of *Helicobacter pylori* [2,3]. Intestinal metaplasia in stomach is typically classified into two types: mixed gastric-and-intestinal type (incomplete type) and solely intestinal type (complete type) [4]. In the process of metaplastic change of gastric mucosa, induction of intestinal differentiation and loss of gastric differentiation occur simultaneously or asynchronously [5,6].

For induction of intestinal differentiation, we and other groups have been reported that Cdx must be an indispensable key molecule by regulating transcription of many intestinal marker

genes [7,8,9,10,11,12,13]. On the contrary, the molecular mechanism of loss of gastric genes in the process of metaplastic change in stomach remains poorly understood. It is probably due to inadequate identification of gastric marker genes, and also due to unsolved expression regulation of these gastric genes. Based on these backgrounds, we focused on *MUC5AC*, which is a well-established gastric marker gene [6,14] and is often used for the clinical assessment of gastric cancer [15]. There have been many previous reports investigating the expression of *MUC5AC* and prognosis of gastric cancer, but the association between expression of *MUC5AC* and malignant potential of gastric cancer is still controversial [16,17,18,19]. Nevertheless, *MUC5AC* is one the most evident gastric marker clearly decreased in the process of intestinal metaplasia [14,20]. We believe elucidating the mechanism of *MUC5AC* gene expression in gastrointestinal cells must be useful to understand the loss of gastric differentiation during the development of pre-malignant atrophic gastritis.

Our aim of this study is to find a critical mechanism of *MUC5AC* expression regulation in human gastrointestinal cells. To date, HIF-1α [21], Smad4 [21,22], Sp1 [22], GATA-4/-6, and HNF-1/-4 [23] are reported to activate murine *MUC5AC*. Sp1 and Gli are reported to enhance *MUC5AC* expression in human lung-epithelial and pancreatic cancer cells, respectively [24,25]. Contrastively, ATBF1 is negatively regulate *MUC5AC* expression in human gastric cancer cells [26], In spite of these results, molecular mechanisms of MUC5AC expression in human gastrointestinal cells have not been fully elucidated. In the present study, we identified 15 bp sequence in human *MUC5AC* 5′-flanking region which plays an important role in *MUC5AC* expression in gastrointestinal cancer cells, and also found that the region contains a putative Gli-binding site which does not coincide with previous report [25]. Gli is one of transcriptional factors which has a DNA binding zinc finger domain [27]. In this study, we examined molecular roles of Gli on *MUC5AC* promoter in gastrointestinal cells. Our results demonstrated that *MUC5AC* expression depends on cooperative regulatory mechanism of Gli, some epigenetic modulation, and other factors in gastrointestinal cells.

Materials and Methods

Cell Culture

Twenty gastric cancer cell lines, ten colorectal cancer cell lines, and two non-gastrointestinal cancer cell lines were maintained in high-glucose DMEM with 10% fetal calf serum (Gibco/Invitrogen, Carlsbad, CA) at 37°C in a humidified 5% CO_2 atmosphere. Names of used cell lines and histological types of gastric cancer cell lines were described in our previous reports [6]. Human T98G and A172 cell lines were purchased from the RIKEN Bio Resource Center (Tsukuba, Japan). For the treatment with DNA demethylation reagent or histone deacetylase (HDAC) inhibitor, 5-Aza-2′-deoxycytidine (5-Aza-dC, Sigma-Aldrich) at 2 μg/ml and/or trichostatin A (TSA, Sigma-Aldrich) at 25–1000 ng/ml were added to the culture medium.

Tumor Samples

For the advanced gastric cancer specimens, we randomly selected 89 gastric adenocarcinoma samples surgically resected at the Fujita Health University Hospital. For the early stage gastric cancer endoscopically resected, we selected 78 specimens banked at the University of Tokyo Hospital. This study was approved by the ethic committees of the University of Tokyo, and also by the institutional ethical review board for human investigation at Fujita Health University. According to the Declaration of Helsinki, written informed consents were obtained from all the study participants for use of resected sample in research.

Immunohistochemistry

Deparaffinization and endogenous peroxidase inactivation of clinical tissues were performed as described previously [28]. For *MUC5AC*, hydrated heating in 1 mM EDTA buffer (pH 8.0) at 120°C was then performed in a pressure cooker (Delicio 6L; T-FAL, Rumily, France) for 10 min for antigen retrieval. The primary immunostaining with anti-MUC5AC antibody (NCL-MUC-5AC, Novocastra, Newcastle-upon-Tyne, UK) at a 1:200 dilution was applied for 12 hours at room temperature. After washing in PBS three times, the secondary immunostaining with Histofine Simple Stain MAX-PO(G) (Nichirei, Tokyo, Japan) was applied for 30 min at room temperature. Based on the evaluation by the two independent pathologists, ratios of *MUC5AC*-positive cells were classified into four classes: 1) <10%, 2) ≥10% and < 50%, 3) ≥50% and <80%, and 4) ≥80%.

For Gli1 immunostaining, hydrated heating in 10 mM citrate buffer (pH 6.0) was done in a pressure cooker for 10 min for antigen retrieval. The sections were then incubated for 1 h at room temperature with antihuman Gli1 antibody (H-300, sc-20867, Santa Cruz Biotechnology) at a 1:500 dilution. For the amplification of signals, anti-rabbit antibody (Dako, Hamburg, Germany) was applied to the slides for 30 min at room temperature. This was followed by incubation with FITC-conjugated phenol (fluorescyl-tyramide; Dako) for 15 min at room temperature and incubation with anti-FITC antibody conjugated to HRP (Dako) for 15 min at room temperature was then done.

Plasmid constructions

The primer sequences used in plasmid constructions are listed in Table 1. To construct the vectors for luciferase reporter assays, the 2000 bp and 1433 bp of *MUC5AC* promoter region were amplified from TIG-112 genome using the primers MUC5A-Cup-F-01/MUC5ACup-R-01 and MUC5ACup-F-02/MUC5A-Cup-R-01. The amplified products were cloned into pT7blue-T-vector (Novagen, Darmstadt, Germany), and then digested with SalI and BamHI. The excised 2 kb and 1.4 kb DNA fragments were inserted into the XhoI/BglII site of pGL4.12 (Promega, Madison, WI, USA) to generate pGL4.12-hMUC5ACup2000bp and pGL4.12-hMUC5ACup1433bp. NcoI-HindIII fragment from pGL4.12-hMUC5ACup2000bp was inserted into the EcoRV/HindIII site of pGL4.12 to generate pGL4.12-hMUC5A-Cup451bp. The 280 bp, 190 bp, 158 bp, 150 bp, 138 bp, 125 bp and 110 bp of *MUC5AC* promoter region were amplified from pGL4.12-hMUC5ACup451bp as a template using primers MUC5ACup-280-XhoI, MUC5ACup-190-XhoI, MUC5ACup-158-XhoI, MUC5ACup-150-XhoI, MUC5ACup-138-XhoI, MUC5ACup-125-XhoI, MUC5ACup-110-XhoI and pGL412-HindIII, digested with HindIII and XhoI, and inserted into the HindIII/XhoI site of pGL4.12 to generate pGL4.12-hMUC5A-Cup280bp, pGL4.12-hMUC5ACup190bp, pGL4.12-hMUC5A-Cup158bp, pGL4.12-hMUC5ACup150bp, pGL4.12-hMUC5A-Cup138bp, pGL4.12-hMUC5ACup125bp and pGL4.12-hMUC5ACup110bp. The 4010 bp to 1432 bp upstream of MUC5AC promoter region was amplified from genome of TIG-112 genome using the primers MUC5ACup-SacI-F and MUC5A-Cup-PciI-R, digested with SacI and PciI, and inserted into the SacI/PciI site of pGL4.12-hMUC5ACup2000bp to generate pGL4.12-hMUC5ACup4010bp. The 3000 bp to 1432 bp upstream of MUC5AC promoter region was amplified from TIG-112 genome using the primers MUC5ACup-3000-NheI-F and MUC5ACup-PciI-R, digested with NheI and PciI, and inserted

into the NheI/PciI site of pGL4.12-hMUC5ACup2000bp to generate pGL4.12-hMUC5ACup3000bp. To delete the 15 bp in the *MUC5AC* promoter region (125 bp to 111 bp upstream), PCR-based mutagenesis was performed using primers MUC5A-Cup-15delete-F and MUC5ACup-15delete-R and cloned into pGL4.12 to generate pGL4.12-hMUC5ACup451bp-delta15bp. The plasmid was confirmed by sequence analysis. The 284 bp SbfI-HindIII region of pGL4.12-hMUC5ACup4010bp was replaced by the 269 bp SbfI-HindIII fragment of pGL4.12-hMUC5ACup451bp-delta15bp to generate pGL4.12-hMUC5A-Cup4010bp-delta15bp.

Gli1 and Gli3 cDNAs were purchased from Open Biosystems (clone ID 3531657 and 40125719, respectively, Huntsville, AL,) and Gli2 cDNA (pENTR223.1-hGli2) was purchased from DNAFORM K.K. (clone ID 100069128, Yokohama, Japan). EcoRI-XhoI fragment containing Gli1 cDNA was inserted into the EcoRI/XhoI site of pMXs-IP to generate pMXs-Gli1-IP. EcoRI-EcoRV fragment containing Gli3 cDNA was inserted into the EcoRI/PacI site of pMXs-IP to generate pMXs-Gli3-IP. XbaI-NotI fragments from pMXs-Gli1-IP and pMXs-Gli3-IP were inserted into the NheI/NotI site of pcDNA3.1(+) to generate pcDNA3.1(+)-Gli1 and pcDNA3.1(+)-Gli3. BsrGI-AvrII fragment from pENTR223.1-hGli2 was inserted into the Acc65I/XbaI site of pcDNA3.1(+) to generate pcDNA3.1(+)-Gli2.

Luciferase reporter assay

Cells were cultured on 96-well plates and transiently transfected with mixtures of Renilla luciferase control vector pGL4.74 (Promega) (15 ng) and the firefly luciferase reporter plasmids (150 ng) by using Lipofectamine and Lipofectamine PLUS (Invitrogen). To examine the effect of Gli on the promoter activities, pcDNA3.1(+)-Gli1, -Gli2, and -Gli3 plasmids were transfected with pGL-based plasmids at the same time. Luciferase assays were performed at 24 or 48 h post-transfected using the Dual luciferase reporter assay system (Promega). Luciferase activities were measured by an AutoLumat Plus LB953 (Berthold, Bad Wildbad, Germany). Luciferase activity was normalized to a Renilla control and the results are shown as mean ± SD from at least three independent experiments.

Production and infection of retrovirus vectors

pMXs-Gli1-IRES-Puro, pMXs-Gli2-IRES-Puro and pMXs-Gli3-IRES-Puro and control vector (pMXs-IRES-Puro) were transfected with pCAG-VSVG into the PLAT-GP packaging cell line for retrovirus vector production (Cell Biolabs, Inc. San Diego, CA) using Lipofectamine and Lipofectamine PLUS (Invitrogen). Virus-containing supernatants were harvested at 24 h, 48 h and 72 h post-transfection, pooled, and filtered though a 0.45-μm filter (Millipore, Bedford, MA). To assess the effects of overproduction of Gli, cells were infected by adding retrovirus-containing supernatant at a final concentration of 8 μg/ml Polybrene (Sigma) and were selected over 3 days with puromycin (Sigma).

Transfection

Cells were transiently transfected with pcDNA3.1(+)-Gli1, pcDNA3.1(+)-Gli2, pcDNA3.1(+)-Gli3 and pcDNA3.1(+) plasmids for 24–48 h using Lipofectamine and Lipofectamine PLUS, and were used for RT-PCR and luciferase reporter assay.

RT-PCR

Total cellular RNA was prepared using the Isogen RNA isolation reagent (Wako Pure Chemical Industries, Osaka, Japan) as previously reported [29]. RT-PCR was performed via a Superscript One-Step reaction using the Platinum Taq (Invitrogen). The primer sequences used for RT-PCR are shown in Table 2. RNA was reverse-transcribed for 30 min at 50°C, and after an initial denaturation at 94°C for 3 min, cDNA amplification procedures were performed as follows: for *MUC5AC*, 35 cycles of 94°C for 30 sec, 64°C for 1 min, and 72°C for 1 min; for *GAPDH*, 30 cycles of 94°C for 30 sec, 60°C for 1 min, and 72°C for 1 min; for *Gli1* and *Gli2*, 35 cycles of 94°C for 30 sec, 60°C for 1 min, and 72°C for 1 min; for *Gli3*, 40 cycles of 94°C for 30 sec. A commercial RNA panel, Human Total RNA Master Panel II, was purchased from Clontech Laboratories (Palo Alto, CA, USA).

siRNA

SH-10-TC cells were transfected with siGENOME SMARTpool siRNA against human Gli1 and/or Gli2 (M-003896-00-0005 and M-006468-02-0005, respectively; Dharmacon, Lafayetta, CO, USA) using Lipofectamine RNAiMAX (Invitrogen) according to the manufacture's instructions. RNA was extracted from the cells 48 h after siRNA transfection and used for RT-PCR.

Chromatin immunoprecipitation (ChIP) assay

ChIP analyses were performed using a ChIP assay kit (Upstate Biotechnology Inc., Lake Placid, NY) according to the manufacture's instructions. For crosslinking, cells (2×10^6) were incubated at 37°C for 15 min in PBS containing 1% formaldehyde. Cells were collected after two washes with ice-cold PBS and subjected to centrifugation for 5 min at 700×g. Cells pellets were resuspended 400 μl sodium dodecyl sulfate (SDS) lysis buffer (ChIP assay kit, Upstate) containing protease inhibitors (0.1 M phenylmethylsulfonylfluoride and 4 μl protease inhibitor cocktail (Sigma)), and incubated for 10 min on ice. DNA was sonicated (setting 5, Handy Sonic, model UR-20P; Tomy Seiko, Co., Ltd., Tokyo, Japan) and then subjected to centrifugation at 13,000 rpm for 10 min. Supernatants were diluted 10-fold with Chip dilution buffer (ChIP assay kit, Upstate). 1% of the supernatant was retained as the

Table 1. Primers used for plasmid constructions.

Name	Sequence
MUC5ACup-F-01	5′-attcattcacccattcactcactcattcac-3′
MUC5ACup-F-02	5′-tgccacatgtgaagtgctctttctctaggc-3′
MUC5ACup-R-01	5′-tgtgtggacggcggggaagagtgccctgtc-3′
MUC5ACup-280-XhoI	5′-taggctcgagtatgtggggaggacccctgc-3′
MUC5ACup-190-XhoI	5′-cgccctcgagcggccgctggccagcccgca-3′
MUC5ACup-158-XhoI	5′-gagcctcgagtgtttacttgggtgaggggg-3′
MUC5ACup-110-XhoI	5′-gcccctcgaggtgaagcacggggctggagc-3′
MUC5ACup-150-XhoI	5′-actgctcgagtgggtgaggggggaaccacag-3′
MUC5ACup-138-XhoI	5′-ggtgctcgagaaccacaggccccgccctgc-3′
MUC5ACup-125-XhoI	5′-cacactcgaggccctgcccacccacgtgaa-3′
pGL412-HindIII	5′-ccggattgccaagcttggcc-3′
MUC5ACup-SacI-F	5′-tgcccacagagctcagaaacaaggc-3′
MUC5ACup-PciI-R	5′-agagcacttcacatgtggcaggagt-3′
MUC5ACup-3000-NheI-F	5′-acttgctagctcatacactcattcacttat-3′
MUC5ACup-15delete-F	5′-gagggggaaccacaggccccgtgaagcacggggctggagc-3′
MUC5ACup-15delete-R	5′-gctccagccccgtgcttcacggggcctgtggttccccctc-3′

doi:10.1371/journal.pone.0106106.t001

Table 2. Primer pairs, annealing temperatures (Tm), and product sizes (Length) for the 5 genes analyzed by RT-PCR.

Genes		Forward (F) and reverse (R) primer sequences	Tm(°C)	Length
MUC5AC	F	5′-accggtgccacatgacggac-3′	64	396
	R	5′-acgtggccgcctcacacgtg-3′		
Gli1	F	5′-gaaggagttcgtgtgccact-3′	60	491
	R	5′-gtctgctttcctccctgatg-3′		
Gli2	F	5′-gcaacaaagccttctccaac-3′	60	430
	R	5′-atctccacgccactgtcatt-3′		
Gli3	F	5′-aaagcaaacaggagcctgaa-3′	60	401
	R	5′-ggaatgcgttctgttttggt-3′		
GAPDH	F	5′-accacagtccatgccatcac-3′	60	423
	R	5′-tccaccaccctgttgctgta-3′		

doi:10.1371/journal.pone.0106106.t002

input, and the rest was then subjected to immunoprecipitations. Immunoprecipitations were performed overnight at 4°C with 3 μg of anti-Gli1 antibody (H-300, sc-20687; Santa Cruz Biotechnology, Santa Cruz, CA) and nonimmunized rabbit IgG whole molecule (sc-2027; Santa Cruz Biotechnology). After reverse crosslinking, the obtained DNA was purified using PCR product purification kit (Qiagen, Valencia, CA, USA). Immunoprecipitated DNA was analyzed by PCR using primers 5′-ctcggaaactgggctctacccgg-3′ and 5′-gagctttttgtagccccagagctgg-3′ to amplify a fragment of the *MUC5AC* promoter region. Primer pairs for the *villin 1* promoter region were used as a negative control [8].

Results

Decrease of MUC5AC expression accompanied with progression of gastric canceration

To evaluate the expression of MUC5AC in gastric cancer, immunostaining was performed using the clinical specimen representing three-grade gastric epithelial cells from the view of tumorigenesis: non-tumorous but precancerous cells of atrophic mucosa around early gastric cancer (Fig. 1A), malignant cells of early gastric cancer endoscopically resected (Fig. 1B), and malignant cells of advanced gastric cancer surgically resected (Fig. 1C). Our results revealed that the stronger the malignant property of gastric epithelial cells is, the weaker the expression of MUC5AC is. In other word, expression of MUC5AC decreases accompanied with increased malignant property of gastric mucosa.

Some previous studies including ours reported that expression of MUC5AC often attenuates during the development of pre-malignant intestinal metaplasia [6,14]. Our present data further showed that decrease of MUC5AC expression advances in the process of gastric canceration. From these results, we are convinced that it is important to elucidate the regulatory mechanism of *MUC5AC* gene expression for understanding tumorigenesis of gastric cancer.

A highly conserved region containing a Gli-binding sequence (HCR-Gli) is present in the promoter of *MUC5AC* gene

To examine the transcriptional regulation of *MUC5AC* gene, the upstream 5′-flanking regions of *MUC5AC* gene of 13 mammal species retrieved from GenBank (dated 8 May, 2013) were aligned using ClustalW (ver 2.1) sequence alignment program [30]. The major transcription initiation site of human *MUC5AC* gene has been mapped to 48 bp upstream of the ATG translation start site [31]. Alignment of the human sequence with other mammal sequences denoted high homology among orthologs within ~200 bp upstream of the ATG start codon (Fig. 2).

To test the function of the conserved promoter regions identified above, a series of luciferase reporter constructs containing 451 bp or shorter fragments of the human *MUC5AC* promoter region were generated. Promoter activities of these deletion constructs were measured by luciferase reporter assay in the three *MUC5AC*-expressing cell lines derived from human gastrointestinal cancer: SW480, SH-10-TC, and KE-39 [6]. As shown in Fig. 3A, the promoter activity of the reporter construct containing upstream 110 bp was much lower than those containing upstream 451, 280, 190, and 158 bp.

To examine the essential region for the luciferase activity between −158 to −110 bp more precisely, reporter constructs containing 150, 138, and 125 bp upstream of ATG start codon were generated and examined their activities (Fig. 3B). Although the reporter constructs containing upstream 158, 150, 138, and 125 bp showed high luciferase activities, the construct containing upstream 110 bp denoted very low activities equal to a negative control.

Next we made a deletion mutant construct containing upstream 451 bp but lacking the region between −125 and −111 bp, and examined the promoter activity (Fig. 3C). Deletion of the 15 bp led to a marked decrease in the luciferase activity, suggesting that the 15 bp sequence between −111 to −125 bp is critical for the *MUC5AC* promoter activity. Based on the thorough literature search [32,33,34,35,36,37,38], we found a putative Gli-binding site in this short 15 bp sequence (5′-GCCCTGCCCACCCAC-3′ shown in Fig. 3D). We could not find any other transcription factors which bind to this 15 bp sequence by searching transcription factor database. Consequently, we named this 15 bp sequence as a highly conserved region containing a Gli-binding site (HCR-Gli).

Exogenous modulation of Gli affects the endogenous *MUC5AC* gene expression in gastrointestinal cells

We examined whether Gli1 can upregulate *MUC5AC* transcription activity in gastrointestinal cell lines. We constructed a retrovirus vectors carrying the *Gli1* gene, and transduced it into four gastric (SH-10-TC, MKN1, NCI-N87, AZ-521), one colorectal (WiDr), and three other cancer cell lines (MDA-

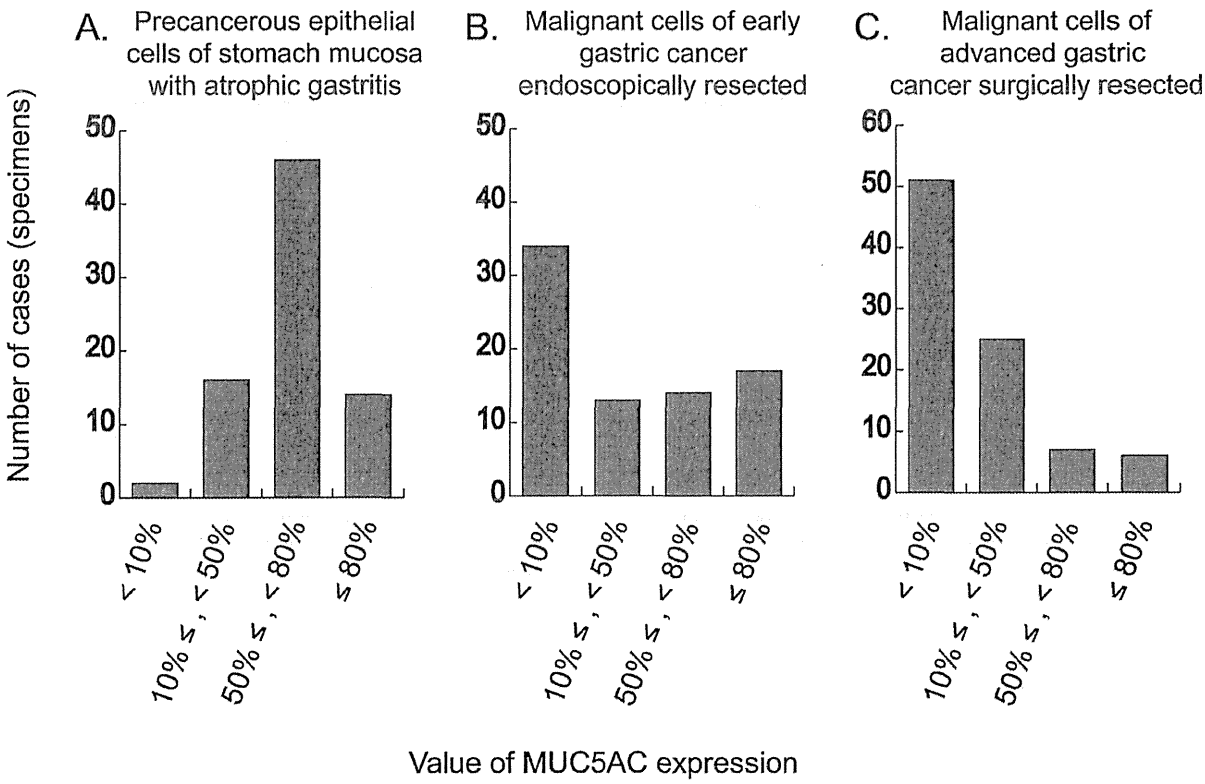

Figure 1. Expression of MUC5AC in non-tumorous epithelial cells of atrophic mucosa around early gastric cancer endoscopically resected (A), malignant cells of early gastric cancer endoscopically resected (B), and malignant cells of advanced gastric cancer surgically resected (C). Based on the percentages of cells with immunoreactivity of MUC5AC, the 78 non-malignant or malignant specimens (A, B) and 89 malignant specimens (C) were classified into four categories: 1) <10%, 2) ≥10% and <50%, 3) ≥50% and <80%, and 4) ≥80%.
doi:10.1371/journal.pone.0106106.g001

MB435, T98G, A172). In the resulting stable transductants, the expression levels of *MUC5AC*, *Gli1*, and *GAPDH* were analyzed by RT-PCR (Fig. 4A). Although there were two exceptions of AZ-521 and WiDr, *MUC5AC* was found to be universally upregulated by Gli1 overexpression.

We next compared the three Gli homologs (*Gli1*, *Gli2*, and *Gli3*) identified in human. To examine the effect of these transcription factors on *MUC5AC* expression, AGS and SW480 cell lines transiently overexpressing Gli1, Gli2 and Gli3 were analyzed by RT-PCR (Fig. 4B). Gli1 strongly upregulated *MUC5AC* expression, which was consistent with the result of stable transductants in Fig. 4A. Gli2 and Gli3 also increased the *MUC5AC* expression, but their effects were weaker than Gli1.

To address whether Gli1, Gli2, and Gli3 activate the *MUC5AC* promoter through the 15 bp of HCR-Gli, we performed the luciferase reporter assay using the construct containing upstream 451 bp of the human *MUC5AC* gene and the deletion mutant lacking the HCR-Gli (Fig. 4C). In the *Gli*-transfected SW480, SH-10-TC, and KE-39 cells, all the three Gli homologs enhanced activation of the reporter construct containing upstream 451 bp of *MUC5AC*, but not of the deletion mutant lacking the HCR-Gli. These results indicate that Gli1, Gli2, and Gli3 can efficiently activate *MUC5AC* transcription through the HCR-Gli. From these results, we speculate that Gli1, Gli2 and Gli3 may play redundant roles but the effect of Gli1 is stronger than that of others upon the upregulation of *MUC5AC* expression.

We next examined the effect of Gli knockdown by siRNA transfection on *MUC5AC* expression. After SH-10-TC cells were transfected with Gli1 and/or Gli2 siRNA, the expression levels of *MUC5AC*, *Gli1*, *Gli2*, and *GAPDH* were analyzed by RT-PCR. As shown in Fig. 4D, double knockdown of Gli1 and Gli2 most efficiently decreased *MUC5AC* expression, whereas the effects of either Gli1 or Gli2 single knockdown were considerably weaker. These results suggest that Gli1 and Gli2 have redundant functions for *MUC5AC* expression, which is consistent with our above-mentioned speculation.

Gli interacts to HCR-Gli in the *MUC5AC* promoter region

To determine whether Gli1 directly binds to the *MUC5AC* promoter, chromatin immunoprecipitation (ChIP) assays were performed using anti-Gli1 antibody. As a negative control, the human *villin1* promoter sequence was used because *villin1* is a typical intestinal marker gene regulated by Cdx [8], and also because exogenous modulation of Gli1 expression level did not change endogenous *villin1* expression (our unpublished observation). As shown in Fig. 4E, the HCR-Gli-containing fragment of *MUC5AC* promoter was co-immunoprecipitated with Gli1 in SW480 and KE-39 cells, whereas the upstream sequence of *villin1* promoter was not. Our results demonstrate that Gli1 activates *MUC5AC* gene transcription through direct interaction between Gli1 and the *MUC5AC* promoter region.

Taking all the results from luciferase assays with upstream deletion constructs, overexpression and knockdown of Gli, and

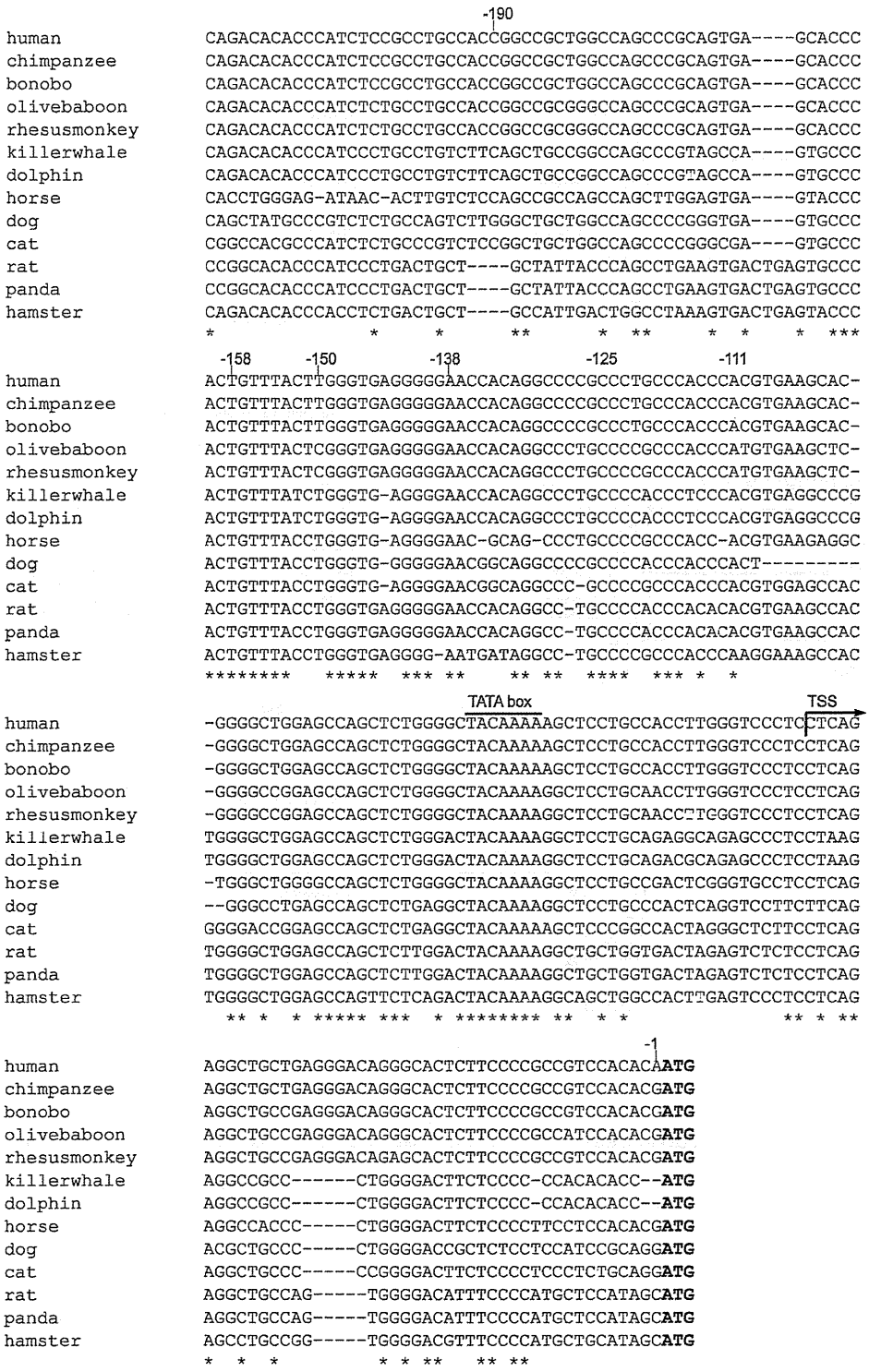

Figure 2. Comparison of the 5′-upstream sequences of *MUC5AC* gene of 13 mammal species. Alignment was carried out using the ClustalW (ver 2.1). The translational start site (TSS, arrow) and the translational starting codon (ATG, bold) are indicated. Asterisks (*) represent exact matches in all the sequences.
doi:10.1371/journal.pone.0106106.g002

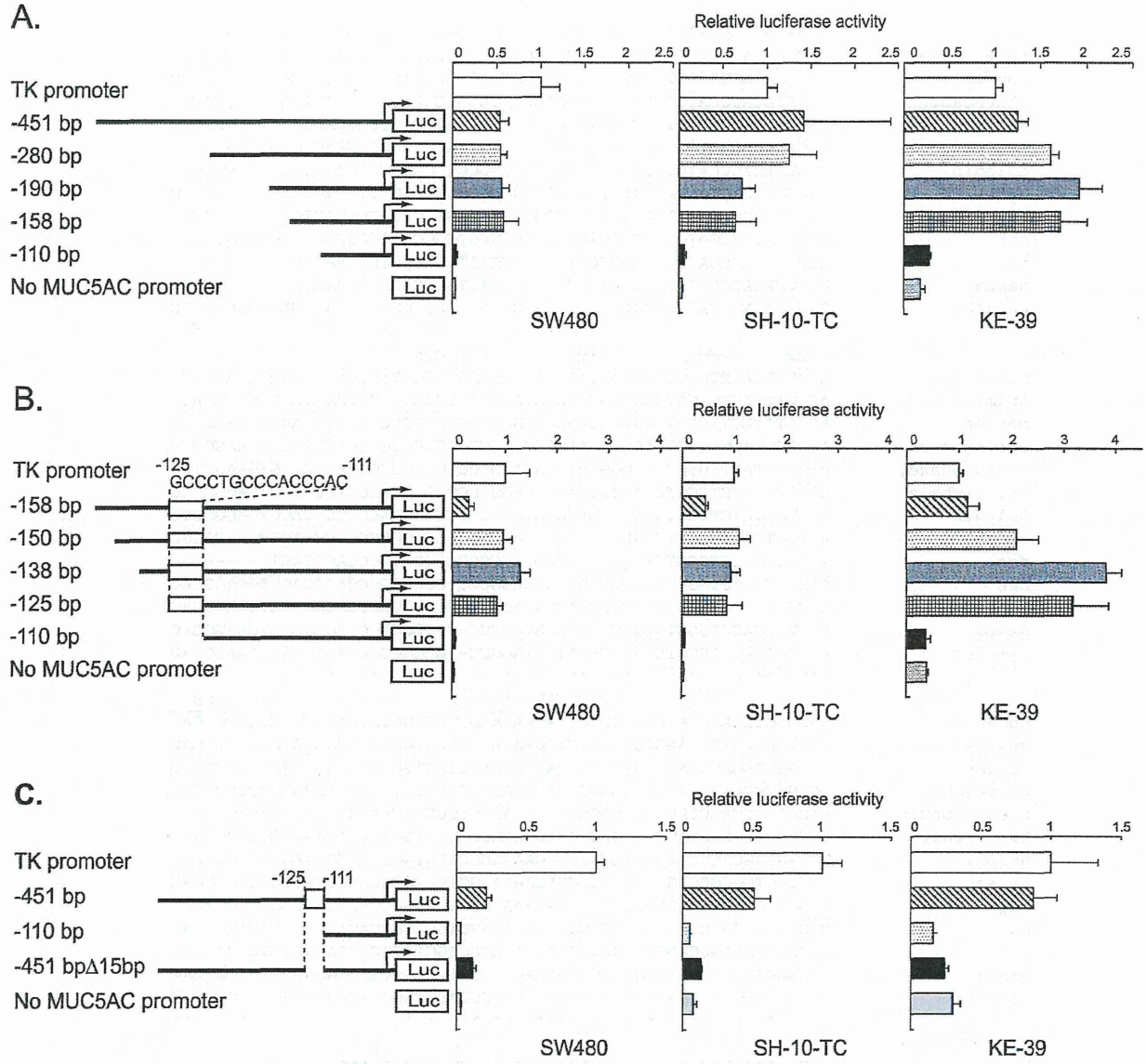

D.

5'-GCCCTGCCCACCCAC-3' (upstream 125~111bp sequences of human *MUC5AC* gene)

5'-GACCACCCA-3'	Kinzler KW, *et al. Mol Cell Biol.* 1990;10:634
5'-GAACACCCA-3'	Yoon JW, *et al. J Biol Chem.* 2002;277:5548.
5'-CACCACCCA-3'	Yoon JW, *et al. J Biol Chem.* 2002;277:5548.
5'-GACCACCCA-3'	Zhu H, *et al. Curr Genomics.* 2010;11:238.
5'-GACCACCAA-3'	Xu XF, *et al. J Carcinog.* 2009;8:13.
5'-GGCCACCCA-3'	Bien-Willner GA, *et al. Hum Mol Genet.* 2007;16:1143.
5'-GGCCACCCA-3'	El-Zaatari M, *et al. PLoS ONE.* 2013;8:e58935.
5'-GATCATCCA-3'	Wang F, et al. *PLoS ONE.* 2011;6:e18434

Figure 3. Luciferase reporter analyses of a series of *MUC5AC* promoter constructs in gastrointestinal cell lines and identified highly conserved sequence similar to known Gli-binding sequences. (A–C) Data represent the mean of luciferase activities of SW480, SH-10-TC, and KE-39 cells measured at 24 h after transfection. The error bars showed the standard deviation of the results from three independent experiments. (D) Alignment of the highly conserved sequence in *MUC5AC* promoter region with previous reported sequences of Gli-binding site.
doi:10.1371/journal.pone.0106106.g003

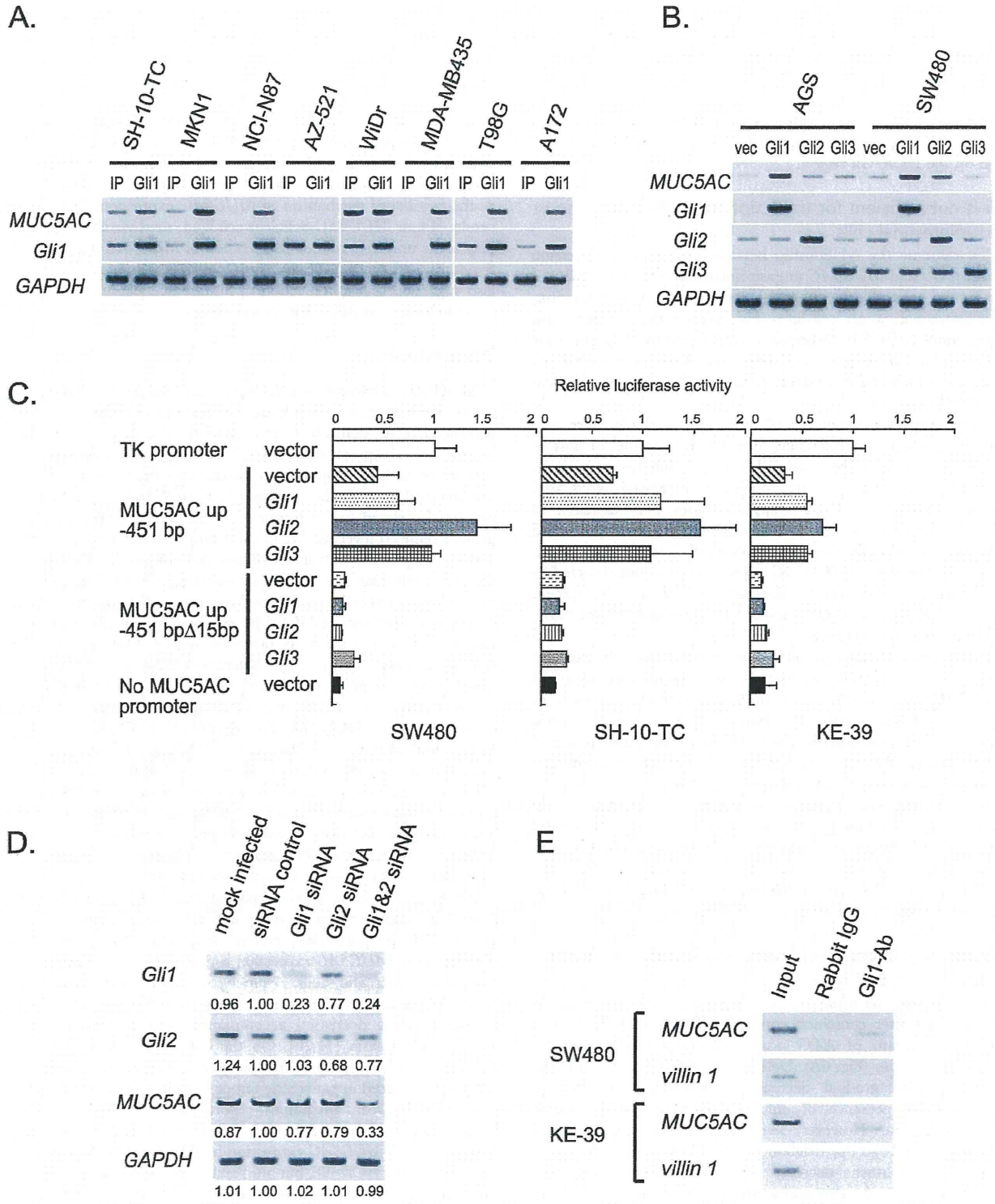

Figure 4. Effects of exogenous modulation of Gli on *MUC5AC* gene expression. (A) RT-PCR detecting *MUC5AC* mRNA in 5 gastrointestinal and 3 non-gastrointestinal cell lines infected with retroviral vector encoding *Gli1* gene. (B) RT-PCR detecting *MUC5AC* mRNA in AGS and SW480 cells transfected with pcDNA3.1(+) (vec), pcDNA3.1(+)-Gli1, pcDNA3.1(+)-Gli2 or pcDNA3.1(+)-Gli3. (C) Luciferase reporter analysis of *MUC5AC* promoter constructs in SW480, SH-10-TC, and KE-39 cells transfected with pcDNA3.1(+) (vector), pcDNA3.1(+)-Gli1, pcDNA3.1(+)-Gli2 or pcDNA3.1(+)-Gli3. (D) *MUC5AC* expression analyzed by RT-PCR using SH-10-TC cells transfected with control siRNA, Gli1 siRNA alone, Gli2 siRNA alone, or Gli1 and Gli2

siRNA. (E) ChIP analyses of the human *MUC5AC* gene in SW480 and KE-39 cells. Anti-Gli1 antibody (Gli1-Ab) and non-immunized rabbit IgG whole molecule were used for immunoprecipitation. PCR was performed with primers recognizing the HCR-Gli-containing fragment of *MUC5AC* promoter or recognizing the promoter region of *villin1* gene.
doi:10.1371/journal.pone.0106106.g004

ChIP analyses into consideration, we concluded that Gli enhances the *MUC5AC* gene transcription via direct protein-DNA interaction on the HCR-Gli region.

Gli is not sufficient for transcription of *MUC5AC* gene in gastrointestinal cells

To examine the relationship between endogenous expression levels of *Gli* and *MUC5AC* in gastrointestinal cells, RT-PCR was performed using the twenty gastric, ten colorectal, and two non-gastrointestinal cancer cell lines (Fig. 5A). All the cell lines with endogenous *MUC5AC* expression were found to be positive for *Gli1* and/or *Gli2* expression. Conversely, there were several cell lines in which *Gli1* and/or *Gli2* were expressed whereas *MUC5AC* was not.

Tissue expression patterns of *MUC5AC* and *Gli* were also examined using a commercially available RNA panel of normal human tissues (Fig. 5B). Although several adult tissues such as stomach, lung, trachea, etc. obviously expressed *MUC5AC* mRNA, about half of the analyzed tissues were deficient in *MUC5AC* expression. On the other hand, *Gli1*, *Gli2*, and *Gli3* were ubiquitously expressed in almost all the examined tissues. It should be noted that *MUC5AC* expression were not detected in adult brain, kidney, liver, placenta, skeletal muscle, spleen, thymus, thyroid gland, etc., despite the expression of the three *Gli* homolog genes (Fig. 5B).

Using non-malignant gastric tissues derived from the surgical specimens, we further evaluated the protein expression of MUC5AC and Gli1 by immunohistochemistry. As shown in Fig. 5C, Gli1 was weakly but ubiquitously expressed on gastric mucosa, which was different from the spotty immunostaining of MUC5AC. All the gastric tissues derived from the seven surgical specimens showed the same expression pattern.

In total, expression patterns of MUC5AC and Gli clearly support our conclusion that Gli is necessary for *MUC5AC* expression in human gastrointestinal cells. In addition, it is also obvious that expression of Gli is not enough for *MUC5AC* expression, suggesting that other mechanism should work cooperatively on the transcription of *MUC5AC* gene.

Multiple regulatory mechanisms work in the promoter region of *MUC5AC* gene

To analyze the far distal promoter region of *MUC5AC* gene, we generated reporter constructs containing 4010, 3000, 2000, and 1433 bp upstream of ATG start codon and examined their promoter activities (Fig. 6A). Deletion from 4010 bp to 1433 bp region revealed gradual decrease in transcriptional activity, suggesting the presence of enhancer elements in this distal promoter region. However, even in the reporter construct including long 4010 bp, deletion of the 15 bp HCR-Gli region resulted in the drastic decrease of luciferase activity (Fig. 6A). Together, our results demonstrated that there are at least two regulatory elements in the *MUC5AC* promoter region: the 15 bp sequence between −111 bp to −125 bp which critical for the promoter activity, and the wider regulatory region in −4010 bp to −1433 bp which can enhance the promoter activity.

To further examine the possible epigenetic regulation on *MUC5AC* expression, four gastrointestinal cell lines and two glioblastoma cell lines were treated with demethylating agent (5Aza-dC) and/or HDAC inhibitor (TSA). Transcription of *MUC5AC* was slightly upregulated in all the four *MUC5AC*-deficient cell lines (Fig. 6B), suggesting that epigenetic regulation such as methylation and/or histone acetylation additionally works as the regulatory mechanism of *MUC5AC* expression. From the results of four *MUC5AC*-deficient cell lines, methylation seems to play some universal role on suppression of *MUC5AC* expression. Synergistic effects of 5-Aza-dC and TSA in A172 and T98G cells also suggested that modification of histone acetylation may have some influence on *MUC5AC* transcription.

Discussion

MUC5AC, a secreted mucin highly detected in the superficial gastric epithelium, is a well-known gastric marker often used for classification of stomach cancer [20,39]. We have previously reported that expression of *MUC5AC* in stomach decreases in association with development of intestinal metaplasia [6]. In the present study, we further showed that *MUC5AC* expression is apparently related to the tumor stage: advanced gastric cancers present reduced levels of MUC5AC compared with early gastric cancer. Despite the anticipated importance of *MUC5AC* regulation, the molecular mechanisms underlying *MUC5AC* expression in gastrointestinal cells remain poorly understood. In this study, we searched 5′-upstream of *MUC5AC* gene and identified the HCR-Gli at −125/−111 bp in its promoter region. Our overexpression/knockdown analyses and luciferase reporter assays revealed that Gli induced *MUC5AC* expression through the HCR-Gli in gastrointestinal cells. In addition, ChIP analysis showed that Gli1 directly binds to HCR-Gli. The results of RT-PCR using 30 gastrointestinal tumor cell lines and an RNA panel from systemic normal tissues suggested that Gli is necessary but not sufficient for *MUC5AC* expression, which was consistent with the results from immunohistochemistry of clinical specimens. Furthermore, we found that the far distal upstream region from −1433 to −4010 bp enhances the Gli-dependent *MUC5AC* expression, at least partly based on the epigenetic modulation.

Recently, Inaguma *et al.* reported that Gli1 activates the *MUC5AC* promoter through two putative Gli-binding sites (GBS1 and GBS2) in pancreatic cancer cells [25]. However, the significance of *MUC5AC* expression is different in gastrointestinal cells and pancreatic cells. Namely, abundant expression of MUC5AC is observed in normal epithelial cells of stomach but its expression is decreased accompanied with development of intestinal metaplasia [14,20]. On the other hand, *MUC5AC* is generally undetectable in normal pancreas tissue and is sometimes ectopically induced in pancreatic tumor cells. In fact, there are two differences between Inaguma's report and our results. First, Inaguma *et al.* showed that both GBS1 and GBS2 respond to upregulation of *MUC5AC* expression by Gli. The GBS1 overlaps to our identified HCR-Gli, but our results indicated that the GBS2 (corresponding to −159/−168 bp in Fig. 2) has no effect on *MUC5AC* expression (Fig. 3A). Second, Inaguma *et al.* reported that Gli1 expression correlates with MUC5AC induction by immunohistochemistry. However, our results revealed that expression of Gli does not always accompany with *MUC5AC* expression in gastrointestinal cells (Figure 5). These inconsistencies might be due to a difference of originated tissues (pancreatic or gastrointestinal).

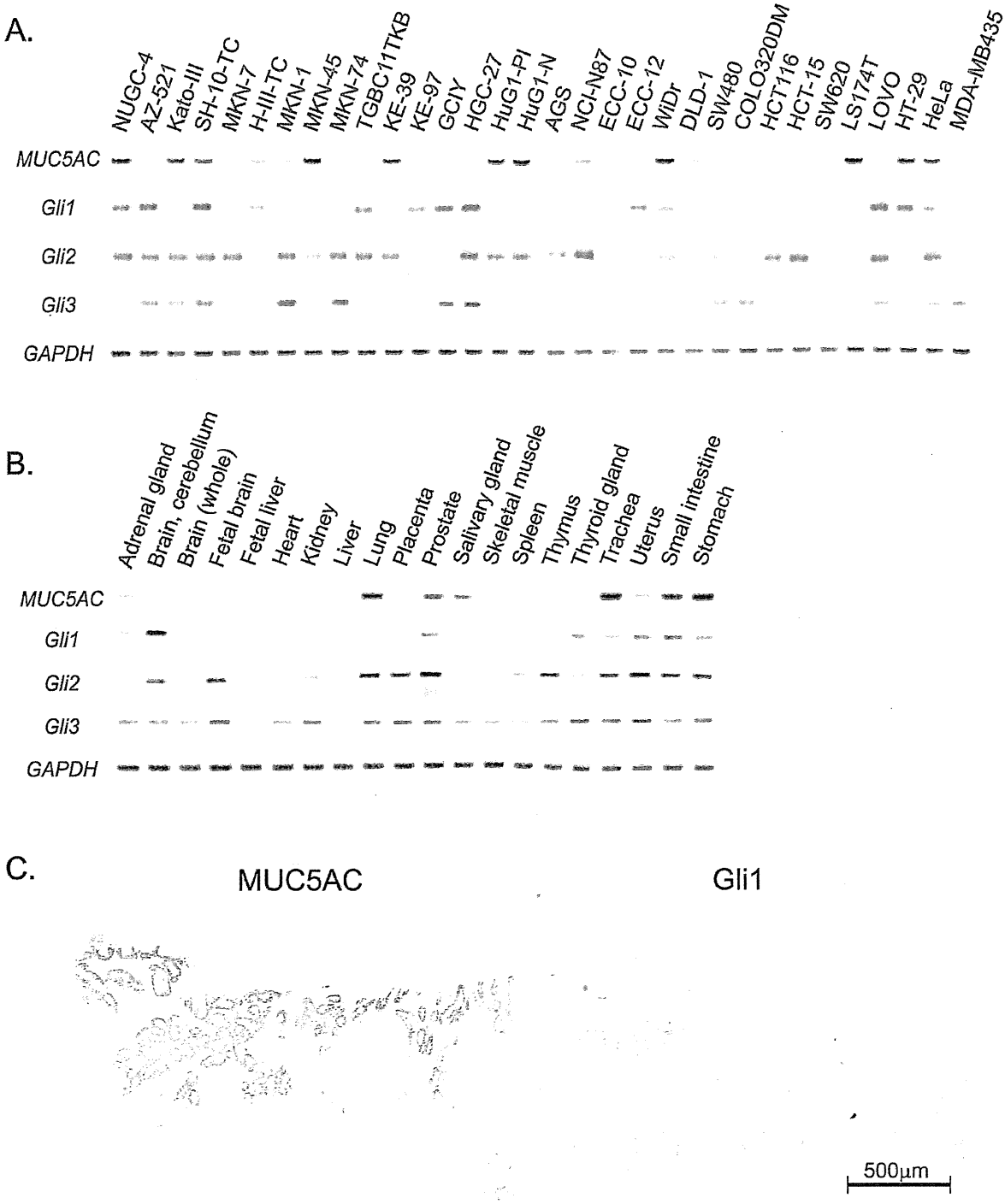

Figure 5. Expression profiles of Gli and MUC5AC in various tumor cell lines and human normal tissues. (A, B) RT-PCR detecting *MUC5AC* and *Gli* homologs in the 30 tumor cell lines (A) and systemic normal tissues (B). (C) Immunostaining of MUC5AC (left panel) and Gli1 (right panel) in sequential sections of non-malignant gastric mucosa.
doi:10.1371/journal.pone.0106106.g005

No induction of *MUC5AC* expression in AZ521 cells (Fig. 4A), which completely lack the SWI/SNF complex-based chromatin remodeling activity [28], may suggest the interaction between Gli and the SWI/SNF complex. Although there have been no previous reports concerning the interaction with Gli, SWI/SNF chromatin remodeling complex has been reported to bind with various transcription factors such as AP-1 [40], CREB [41], MyoD [42], Cdx [8], GATA1 [43], and so on.

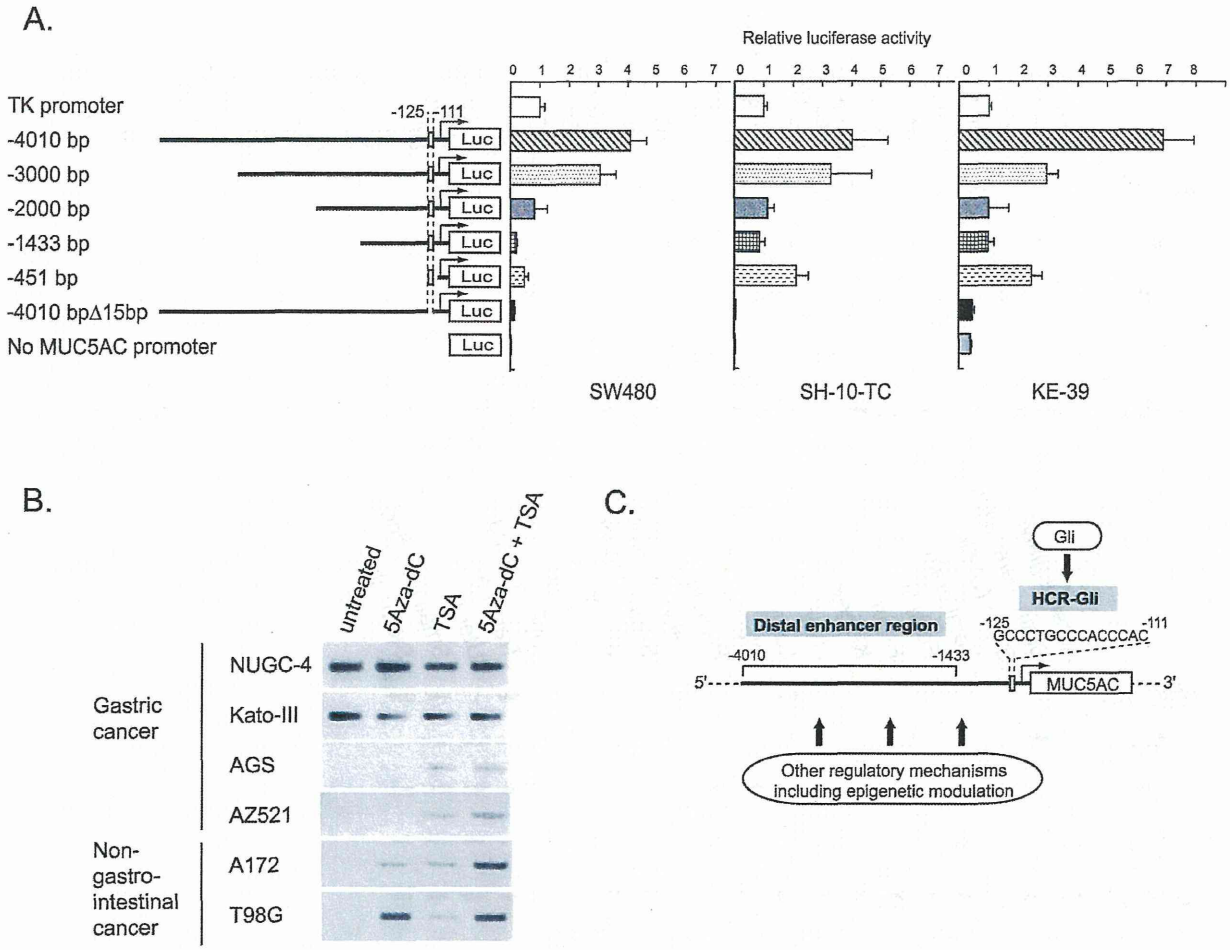

Figure 6. Multiple regulatory mechanisms of *MUC5AC* gene expression. (A) Luciferase reporter analysis of a series of constructs covering the far upstream sequence in the *MUC5AC* promoter. Data represent the mean of luciferase activities in SW480, SH-10-TC, and KE-39 cells measured at 24 h after transfection. The error bars showed the standard deviation of the results from three independent experiments. (B) Expression of *MUC5AC* analyzed by RT-PCR, using the 4 gastric cancer-derived and 2 glioblastoma-derived cell lines treated with 5-Aza-2′-deoxycytidine (5-Aza-dC) and/or trichostatin A (TSA). (C) Schematic representation of the presumed multiple regulations of human *MUC5AC* gene.
doi:10.1371/journal.pone.0106106.g006

The 5′-upstream distal region from −1433 to −4010 bp in *MUC5AC* promoter showed obvious enhancing effect on *MUC5AC* expression (Fig. 6A). Interestingly, we noticed that the region from −1455 to −3187 bp contains 86 copies of tandem sequences 5′-TCA(C/T)TCA(C/T)-3′ (Fig. 6C) [44]. The tandem repeats are conserved among mammals especially among primate and cetartiodactyla. Human, olive baboon, rhesusmonkey, killerwhale, and dolphin have more than 60 repeats of the tandem repeats in their 4010 bp upstream of MUC5AC promoter region. In contrast, horse, dog, cat, panda, and hamster have only less than 10 repeats of the tandem repeats. We have no information for this tandem repeat sequences at present, but it might has some roles on regulation of *MUC5AC* expression.

Recently, Yamada *et al.* showed that the CpG methylation status of around −3.7 kb in the *MUC5AC* promoter is associated with *MUC5AC* expression in some cancer cell lines, suggesting that the expression of *MUC5AC* is epigenetically regulated in the distal promoter region [45]. In fact, we found increase in *MUC5AC* expression by 5Aza-dC and/or TSA treatment, indicating some epigenetic mechanism involved in *MUC5AC* gene regulation (Fig. 6C).

To understand gastric tumorigenesis mainly occurred in the atrophic mucosa with chronic gastritis and intestinal metaplasia, we believe the disrupted balance between intestinal and gastric differentiation must be important [8,28]. For intestinal differentiation, many previous reports indicated that Cdx must be an indispensable key molecule based on the transcriptional regulation of many intestinal differentiation marker genes [8,9,10,11,12]. On the contrary, the critical key molecule for gastric differentiation has not been identified yet. Despite the through screening, we have not found the essential regulator for our identified gastric marker *Cathepsin E* (data not shown) [6], and we have elucidated that typical gastric marker *MUC5AC* gene is partly regulated by Gli, a universal transcription factor which alone cannot realize the tissue-specific expression of *MUC5AC* gene. Unlike intestinal differentiation, we now speculate that gastric differentiation may depend on cooperative regulatory mechanism of some universal transcription factors and epigenetic modulations.